SIAM J. APPL. MATH.
Vol. 70, No. 7, pp. 2119–2149

PARTIAL RESET IN PULSE-COUPLED OSCILLATORS*

CHRISTOPH KIRST† AND MARC TIMME†

Abstract. Pulse-coupled threshold units serve as paradigmatic models for a wide range of complex systems. When the state variable of a unit crosses a threshold, the unit sends a pulse that is received by other units, thereby mediating the interactions. At the same time, the state variable of the sending unit is reset. Here we present and analyze a class of pulse-coupled oscillators where the reset may be partial only and is mediated by a partial reset function. Such a partial reset characterizes intrinsic physical or biophysical features of a unit, e.g., resistive coupling between dendrite and soma of compartmental neurons; at the same time the description in terms of a partial reset enables a rigorous mathematical investigation of the collective network dynamics. The partial reset acts as a desynchronization mechanism. For N all-to-all pulse-coupled oscillators an increase in the strength of the partial reset causes a sequence of desynchronizing bifurcations from the fully synchronous state via states with large clusters of synchronized units through states with smaller clusters to complete asynchrony. By considering inter- and intracluster stability we derive sufficient and necessary conditions for the existence and stability of cluster states on the partial reset function and on the intrinsic dynamics of the oscillators. For a specific class of oscillators we obtain a rigorous derivation of all $N-1$ bifurcation points and demonstrate that already arbitrarily small changes in the reset function may produce the entire sequence of bifurcations. We illustrate that the transition is robust against structural perturbations and prevails in the presence of heterogeneous network connectivity and changes in the intrinsic oscillator dynamics.

Key words. biological neural networks, synchronization, pulse-coupled oscillators, partial reset, cluster states

AMS subject classifications. 37G15, 92B25, 37G40, 37G35

DOI. 10.1137/09074749X

1. Introduction.

Networks of pulse-coupled units serve as paradigmatic models for a wide range of physical and biological systems as different as cardiac pacemaker tissue, plate tectonics in earthquakes, chirping crickets, flashing fireflies, and neurons in the brain [13, 12, 49, 8]. In such systems, units interact by sending and receiving pulses at discrete times that interrupt the otherwise smooth time evolution. These pulses may be sound signals, electric and electromagnetic activations, as well as packets of mechanically released stress. Pulses are generated once the state of a unit crosses a certain threshold value (e.g., the mechanical stress of a tectonic plate becomes sufficiently large or the voltage across a nerve cell membrane becomes sufficiently high); thereafter the state of the sending unit is reset.

Synchronization of oscillators is one of the most prevalent collective dynamics in pulse-coupled systems [48, 22, 23, 9, 11, 32, 27, 28, 64]. Often not all units are synchronized but form clusters consisting of synchronized subgroups of units which in turn are phase-locked to other clusters [22, 66, 47, 6, 32, 31, 43, 53, 54].

In neuronal networks, synchronization and clustering of pulses constitute potential mechanisms for effective feature binding. In this paradigm, different information

*Received by the editors January 22, 2009; accepted for publication (in revised form) January 19, 2010; published electronically April 14, 2010. This work was supported by the Federal Ministry for Education and Research (BMBF) through grant 019Q0430 to the Bernstein Center for Computational Neuroscience (BCCN), Göttingen, and through a grant from the Max Planck Society.
http://www.siam.org/journals/siap/70-7/74749.html
†Max Planck Institute for Dynamics and Self-organization (MPIDS), Bunsenstr. 10, 37073 Göttingen, Germany; Bernstein Center for Computational Neuroscience (BCCN), Göttingen; and Fakultät für Physik, Georg-August-Universität, Göttingen (ckirst@nld.ds.mpg.de, timme@nld.ds.mpg.de).

aspects of the same object represented by activity of different nerve cells are pooled together by temporal correlations and in particular due to synchronous firing [60, 61]. However, strong synchronized firing of nerve cells can also be detrimental: synchrony is prominent during epileptic seizures [19, 45] and observed in the basal ganglia during Parkinson tremor [18]. Here mechanisms for desynchronizing neural activity are desirable [63, 44].

To study key mechanisms that may underlie (de)synchronization, e.g., in biological neural networks, analytical tractable models of pulse-coupled oscillators are helpful tools [52, 48, 41, 1, 22, 9, 67, 16]. Here the rise of the state variable of a free oscillatory unit towards the threshold, the unit's *rise function*, characterizes the *subthreshold dynamics*. If after reception of a pulse the state variable of the unit stays below threshold, it is said to receive *subthreshold input*, whereas excitation above the threshold is *suprathreshold*. Mirollo and Strogatz [48] showed that biological oscillators always synchronize their firing in homogeneous networks with excitatory all-to-all coupling if the rise function has a concave shape. The synchronization mechanism they find has two parts: (i) effective decrease of phase differences of units due to subthreshold inputs, and (ii) instant synchronization due to suprathreshold inputs and subsequent reset to a fixed value.

In general, suprathreshold excitation and a subsequent reset is a dominant mechanism for synchronization of pulse-coupled oscillators because input pulses that force nonsynchronized units to cross threshold at nearby times are reset to the same value, leaving the units in the same state or in very similar states afterwards. Although this reset mechanism plays a crucial role in the synchronization process and the coordination of pulse generation times, its implications for the collective network dynamics has, to our knowledge, not been investigated systematically so far: most existing model studies reset the units with suprathreshold inputs to a fixed value independent of the strength of suprathreshold excitation [7, 22, 41, 59, 66, 14, 16, 33]. This results in a complete loss of information about the prior state of the units and makes the dynamics noninvertible. Some other studies consider the opposite extreme: a complete conservation of suprathreshold inputs during pulse sending and reset [33, 9]. Here we aim at closing this gap by presenting and analyzing a model where the reset (and thus the loss of information about the prior state and the strength of suprathreshold excitation) can be varied systematically.

This article is organized as follows: In section 2 we propose a simple model of pulse-coupled oscillators with *partial reset*, where the response to suprathreshold inputs can be continuously tuned and is not an all-or-none effect. To isolate the consequences of this partial reset, we focus on homogeneous systems of all-to-all pulse-coupled oscillators with convex rise function. In section 3 we briefly present the results of numerical simulations and find that the partial reset has a strong influence on the collective network dynamics: Increasing the strength of the partial reset induces bifurcations from the fully synchronous state via states with large clusters of synchronized units through states with smaller clusters to complete asynchrony. We study this transition rigorously by considering the existence and stability of periodic cluster states with respect to intercluster properties in section 3.4 and to intracluster properties in section 3.5. We derive conditions on the partial reset function and the rise function to bound regions of existence and stability of cluster states. In section 3.6 we present a rigorous derivation of $N-1$ bifurcation points for a specific class of oscillators. We demonstrate that the entire sequence of bifurcations may occur for arbitrarily small changes of the reset function, thus underlining the strong impact of partial reset on collective network dynamics. In section 4 we numerically

illustrate that the transition is robust against structural perturbations and prevails in the presence of heterogeneous network connectivity and rise functions with mixed curvature. In section 5 we discuss our results and relate the simple partial reset model to biophysically more realistic neuron models.

Specific aspects of the implications of linear partial resets on synchronization properties for oscillators have been briefly reported in [37, 39].

2. Networks of pulse-coupled units with partial reset. We first propose a class of pulse coupled threshold elements with partial reset and thereafter focus on units that oscillate intrinsically.

2.1. Absorption rule and instant synchronization. We consider N threshold elements, which at time t are characterized by a single real state variable $u_i(t)$ with $i \in \{1, 2, \ldots, N\}$. In the absence of interactions the state variables evolve freely according to the differential equation

$$\frac{d}{dt}u_i = F(u_i) \tag{2.1}$$

with a smooth function $F : \mathbb{R} \to \mathbb{R}$ specifying the intrinsic dynamics of the units. The free dynamics is endowed with an additional nonlinear reset upon reaching a fixed threshold θ from below,

$$u_i\left(t^-\right) = \theta \quad \Rightarrow \quad u_i(t) = \rho, \tag{2.2}$$

where $\rho < \theta$ is the reset value and we used the notation $u_i\left(t^{\pm}\right) = \lim_{s \searrow 0} u_i(t \pm s)$. By an appropriate shift and rescaling of the state variable and its dynamics, we set $\rho = 0$ and $\theta = 1$ without loss of generality.

The units are δ-pulse coupled. If unit j reaches the threshold, a pulse of strength $\varepsilon_{ij} \geq 0$ is sent instantaneously to units i and their membrane potential is increased by an amount ε_{ij},

$$u_j\left(t^-\right) = \theta \quad \Rightarrow \quad u_i^{(1)} = u_i\left(t^-\right) + \varepsilon_{ij}. \tag{2.3}$$

If a unit i crosses the threshold due to a pulse from unit j,

$$u_i\left(t^-\right) + \varepsilon_{ij} \geq \theta, \tag{2.4}$$

it is said to receive *suprathreshold input*. As it crosses the threshold from below it sends a pulse and is reset. Previous models usually reset these units in the same way as if they reached the threshold without this recurrent input, also referred to as the *absorption rule* (e.g., [48]),

$$u_i(t) \geq \theta \quad \Rightarrow \quad u_i\left(t^+\right) = \rho, \tag{2.5}$$

where the total suprathreshold input is lost. As a consequence two or more units initially in different states u_i and simultaneously receiving suprathreshold inputs will all be reset to the same value ρ, making the absorption rule a strong instant synchronizing element of the network dynamics. An alternative considered in previous studies [41, 33] is *total input conservation*,

$$u_i(t) \geq \theta \quad \Rightarrow \quad u_i\left(t^+\right) = \rho + \left(u_i(t) - \theta\right); \tag{2.6}$$

i.e., the total *suprathreshold input charge* $\zeta = u_i(t) - \theta$ is added to the potential ρ after the reset.

2.2. Partial reset. Here we propose a more general model where the reset value is given by a *partial reset function* $R(\zeta)$ that depends on the suprathreshold input charge $\zeta = u_i(t) - \theta$,

$$u_i(t) \geq \theta \quad \Rightarrow \quad u_i\left(t^+\right) = \rho + R\left(u_i(t) - \theta\right). \tag{2.7}$$

We assume that suprathreshold inputs only have excitatory effects and thus give the following definition.

DEFINITION 2.1. *A function $R : \mathbb{R} \to \mathbb{R}$ which is monotonically increasing and satisfies $R(0) = 0$ is called a* partial reset function.

For a *linear partial response* we set

$$R_c(\zeta) = c\zeta \tag{2.8}$$

with the remaining fraction $0 \leq c \leq 1$ of suprathreshold input charge after the reset. For $c = 0$ we recover the absorption rule (2.5), while $c = 1$ corresponds to total charge conservation (2.6).

Motivation for this extension comes from neural networks. Neurons consist of functionally different compartments, including the dendrite and the soma. While synaptic input currents are collected at the dendrite, the electrical pulses are generated at the soma. Additional charges not used to excite a spike may stay on the dendrite and contribute to the membrane potential after being reset at the soma. Due to intraneuronal interactions and the reset at the soma, a part of this suprathreshold input charge may be lost.

DEFINITION 2.2. *A partial reset function R is said to be* neuronal *if $0 \leq R(\zeta) \leq \zeta$ for all $\zeta \geq 0$.*

2.3. The avalanche process. Since the interaction is instantaneous, a pulse generated by unit j may lift other units above threshold simultaneously. These then generate a pulse on their own, and so on. This leads to an avalanche of pulses (cf. Figure 2.1): Units reaching the threshold at time t due to the free time evolution define the triggering set

$$\Theta^{(0)} = \left\{j \mid u_j\left(t^-\right) = \theta\right\}. \tag{2.9}$$

The units $j \in \Theta^{(0)}$ generate spikes which are instantaneously received by all the connected units i in the network. In response, their potentials are updated according to

$$u_i^{(1)} := u_i\left(t^-\right) + \sum_{j \in \Theta^{(0)}} \varepsilon_{ij}. \tag{2.10}$$

The initial pulse may trigger certain other units $k \in \Theta^{(1)} = \left\{k \mid u_k\left(t^-\right) < \theta \leq u_k^{(1)}\right\}$ to spike, etc. This process continues $n \leq N$ steps until no new unit crosses the threshold. At each step $m \in \{2, 3, \ldots, n\}$ the potentials are updated according to

$$u_i^{(m+1)} := u_i^{(m)} + \sum_{j \in \Theta^{(m)}} \varepsilon_{ij}, \tag{2.11}$$

where

$$\Theta^{(m)} = \left\{k \mid u_k^{(m-1)} < \theta \leq u_k^{(m)}\right\}.$$

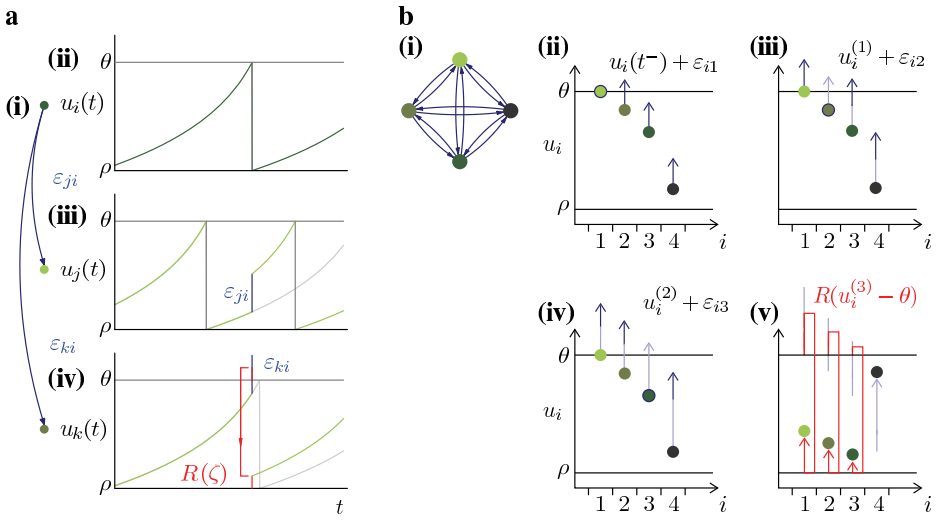

FIG. 2.1. *Model dynamics.* (a) *Sample traces of three units with* (i) *network connectivity* $\varepsilon_{ji} = \varepsilon_{ki} > 0$. (ii) *At time* $t = t_1$ *unit* i *reaches the threshold* θ *and its membrane potential is reset to* ρ. *It generates a pulse which is sent to the units* j *and* k. (iii) *Unit* j *receives the pulse and its membrane potential is increased to* $u_j(t_1^-)+\varepsilon_{ji}$; *the pulse is* subthreshold. (iv) *Unit* k *receives a* suprathreshold *pulse,* $u_k(t_1^-) + \varepsilon_{kj} \geq \theta$, *and its membrane potential is set to* $R(\zeta) = R\left(u_j(t_1^-) + \varepsilon_{kj} - \theta\right)$ *using the* partial reset function R. (b) *Sample avalanche process with* $\Theta = \{1, 2, 3\}$ *and* $n = 3$ *in* (i) *an* $N = 4$ *all-to-all network* $\varepsilon_{ij} = (1 - \delta_{ij})\varepsilon$. (ii) *Unit* $i = 1$ *reaches the threshold* $\Theta^{(0)} = \{1\}$ *and sends a pulse to the other units (arrows). Their potentials are updated to* $u_i^{(1)} = u_i(t^-) + \varepsilon_{i1}$, *causing unit* $i = 2$ *to generate a pulse,* $\Theta^{(1)} = \{2\}$. (iii) *The pulse is received by the other units yielding a potential* $u_i^{(2)} = u_i^{(1)} + \varepsilon_{i2}$ *which brings unit* $i = 3$ *above threshold* $\Theta^{(2)} = \{3\}$. (iv) *The potentials become* $u_i^{(3)} = u_i^{(2)} + \varepsilon_{i3}$ *and no further unit crosses the threshold,* $\Theta^{(3)} = \emptyset$. (v) *The avalanche stops and units that received suprathreshold input are reset to* $u_i(t) = \rho + R\left(u_i^{(3)} - \theta\right)$.

The potentials immediately after the avalanche $\Theta = \bigcup_{q=0}^{n} \Theta^{(q)}$ of size $a = |\Theta|$ are obtained via

$$u_i\left(t^+\right) = \begin{cases} u_i\left(t^-\right) + \sum_{j\in\Theta} \varepsilon_{ij}, & i \notin \Theta, \\ \rho + R\left(u_i\left(t^-\right) + \sum_{j\in\Theta} \varepsilon_{ij} - \theta\right), & i \in \Theta, \end{cases} \tag{2.12}$$

using the partial reset R for units having received suprathreshold inputs.

Note that there is an ambiguity in fixing the precise order of potential updates and resets during an avalanche. Our choice is motivated by neuroscience for the situation where the time scale of the action potential (and subsequent reset) is much faster than the time scale of the synaptic input currents. These in turn should be faster than the time scale of the mechanism reducing the suprathreshold input, e.g., the refractory period (cf. the forthcoming publication [38]). Our model (2.12) then is the limit where all of these time scales become small compared to the time scale of the intrinsic interaction-free dynamics.

For nonzero partial reset functions, potential differences of oscillators involved in a single avalanche will in general not be fully synchronized after the reset. Thus despite the fact that units are generating pulses simultaneously they can have different phases afterwards. We therefore distinguish between *phase synchrony* where units have identical phases and the weaker condition of *pulse synchrony*, which corresponds to simultaneous firing only but allows differences in the phases. When examining the

system with a higher time resolution, phase synchronized units will stay synchronized, whereas pulse synchronized units fire within a short time interval.

2.4. Phase representation of pulse-coupled oscillators with partial reset. In the remainder of this article we will concentrate on units with strictly positive $F > 0$ in (2.1). Then the individual units become oscillatory as the strictly monotonically increasing trajectory $u_i(t)$ of a unit i starting at $u_i(0) = 0$ reaches the threshold after a time T and is reset to zero again. By an appropriate rescaling of time we set $T = 1$. Defining a phase-like coordinate (cf. [48]) via

$$\phi_i(t) = U^{-1}(u_i(t)) := \int_0^{u_i(t)} \frac{1}{F(u)} \mathrm{d}u, \tag{2.13}$$

the interaction free dynamics simplify to

$$\frac{d}{dt}\phi_i(t) = 1. \tag{2.14}$$

By definition U^{-1} is strictly monotonically increasing and has a strictly monotonically increasing inverse U. By our choice of normalization they obey $U^{-1}(0) = 0 = U(0)$ and $U^{-1}(1) = 1 = U(1)$. Note that the function $U(\phi)$ captures the intrinsic rise of the membrane potential towards the threshold, and hence $\phi_i \in S^1 = \mathbb{R}/\mathbb{Z}$ for the phases of the individual units.

DEFINITION 2.3. *A smooth function $U : [0, \infty) \to [0, \infty)$ is called a* rise function *if it is strictly monotonic increasing $U' > 0$ and is normalized to $U(0) = 0$ and $U(1) = 1$.*

DEFINITION 2.4. *Given a rise function U and a partial reset function R, we define for $\varepsilon \geq 0$ the* (subthreshold) interaction function $H_\varepsilon : \left[0, U^{-1}(\theta - \varepsilon)\right) \to S^1$ *by*

$$H_\varepsilon(\phi) := H(\phi, \varepsilon) := U^{-1}(U(\phi) + \varepsilon) \tag{2.15}$$

and the suprathreshold interaction function $J_\varepsilon : \left[U^{-1}(\theta - \varepsilon), \infty\right) \to S^1$ *by*

$$J_\varepsilon(\phi) := J(\phi, \varepsilon) := U^{-1}(R(U(\phi) + \varepsilon - \theta)). \tag{2.16}$$

The pulse-coupling in the potential representation caused by an avalanche Θ at time t, equation (2.12), then carries over to the phase picture as

$$\phi_i(t^+) = \begin{cases} H\left(\phi_i(t^-), \sum_{j\in\Theta} \varepsilon_{ij}\right), & i \notin \Theta, \\ J\left(\phi_i(t^-), \sum_{j\in\Theta} \varepsilon_{ij}\right), & i \in \Theta. \end{cases} \tag{2.17}$$

We remark that $H_\varepsilon^{-1} = H_{-\varepsilon}$.

3. Network dynamics. To identify the effects of the partial reset on the collective network dynamics, we first focus on homogeneous networks consisting of N units with all-to-all coupling and without self-interaction, i.e.,

$$\varepsilon_{ij} = (1 - \delta_{ij})\varepsilon, \tag{3.1}$$

$i, j \in \{1, 2, \ldots, N\}$. We impose the condition $\sum_j \varepsilon_{ij} = (N-1)\varepsilon < \theta - \rho = 1$ to avoid self-sustained avalanches of infinite size.

The analysis of Mirollo and Strogatz [48] shows that in this situation (with a slightly different avalanche process) synchronization from almost all initial conditions is achieved when the rise function is concave ($U'' < 0$) and the absorption rule ($R \equiv 0$) is used. In fact, their result can be generalized to the partial reset model used here and any partial reset function R that is nonexpansive (e.g., $R' \leq 1$). For expansive R the synchronized state no longer has to be the global attractor of the dynamics and typically irregular dynamics is observed. The proof of synchronization for nonexpansive partial resets and the analysis of the bifurcation to the irregular dynamics are presented in a forthcoming study [38].

In this article we concentrate on convex rise functions U, i.e.,

$$\frac{d^2}{d\phi^2} U(\phi) > 0. \tag{3.2}$$

This property holds for a large class of conductance-based leaky-integrate-and-fire (LIF) neurons and a class of quadratic-integrate-and-fire (QIF) neurons (cf. Appendix B). Studying convex rise functions is further motivated by the fact that for these rise functions we already observe a rich diversity of collective network dynamics with a strong dependence on the partial reset R. However, our results also apply to more general rise functions and in particular to sigmoidal shapes as often found for neurons [20, 24].

3.1. Numerical results: A sequence of desynchronizing bifurcations. Systematic numerical investigations indicate a strong dependence of the network dynamics on the partial reset R. In particular, we find synchronous states, cluster states, asynchronous states, and a sequential desynchronization of clusters when increasing the partial reset strength, e.g., by increasing the parameter c when using $R = R_c$.

Starting in the synchronized state and then applying a small perturbation to the phases we observe that the synchronized state is stable for sufficiently small c (Figure 3.1(I)). When the partial reset strength is increased, the synchronized state becomes unstable, and we observe smaller clusters in the asymptotic network dynamics (Figure 3.1(II)), where the final cluster state depends on the precise form of the perturbation. The maximally observed cluster sizes depend on the value of c (Figure 3.2). For sufficiently large c only the asynchronous splay state, i.e., a state with maximal cluster size $a = 1$, is observed (Figure 3.1(III)).

Starting from random initial conditions, we find that for sufficiently small c the synchronous state coexists with a variety of cluster states and the asynchronous state (Figure 3.2). Increasing c, the states involving larger clusters become unstable until finally all random initial conditions lead to the asynchronous state.

What is the origin of this rich repertoire of dynamics, and which mechanisms control the observed transition of sequential desynchronizing bifurcations? To answer these questions, we analytically investigate the existence and stability of periodic states involving clusters of arbitrary sizes $a \leq N$. The following analysis reveals that the sequence of bifurcations is controlled by two effects: subthreshold inputs that are always synchronizing, and suprathreshold inputs that are either synchronizing or desynchronizing, depending on the partial reset strength.

3.2. Strategy of the analysis. We split our analysis of the dynamics into two parts. First we assume that all avalanches are invariant, i.e., the given clusters do not decay into smaller subclusters. This assumption allows us to group all oscillators firing in a single avalanche together into a single "meta-oscillator" with increased firing

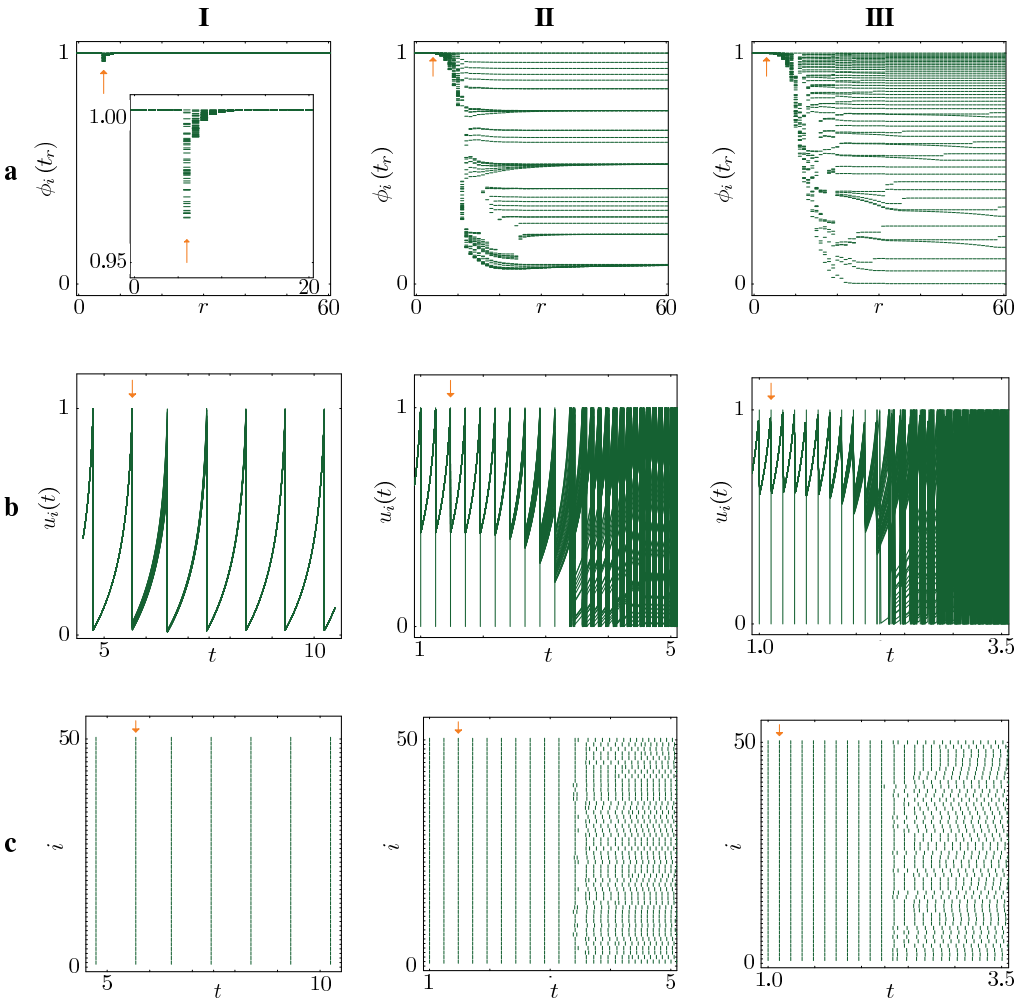

FIG. 3.1. *Desynchronization transition in a network with parameters* $N = 50$, $\varepsilon = 0.0175$, $U = U_b$, $b = -3$, $R = R_c$ *for different values of the partial reset strength:* (I) $c = 0.025 < c_{\mathrm{cr}}^{(N)}$, (II) $c = 0.5 \in (c_{\mathrm{cr}}^{(N)}, c_{\mathrm{cr}}^{(2)})$, *and* (III) $c = 0.7 > c_{\mathrm{cr}}^{(2)}$. *Plotted are* (a) *the phases* $\phi_i(t_r)$ *of all units at pulse generation times* t_r *of the* r*th spike of a reference unit (cf. return map* (3.9)*),* (b) *the potential traces of all units, and* (c) *the raster plots marking the times of pulse generation of each unit* i. *The network is started in the synchronous state, and then a small perturbation is applied at a time indicated by arrows.*

strength and an effective self-interaction. The analysis of the homogeneous all-to-all network ($\varepsilon_{ij} = (1 - \delta_{ij})\varepsilon$) of N oscillators with avalanche sizes a_s, $s \in \{1, 2, \ldots, m\}$, $\sum_s a_s = N$ then reduces to analyzing a network of m meta-oscillators with coupling strengths

$$\varepsilon_{ij} = (1 - \delta_{ij})\varepsilon_i + \delta_{ij}\varepsilon_{ii} \tag{3.3}$$

and $\varepsilon_i = a_i\varepsilon$, $\varepsilon_{ii} = (a_i - 1)\varepsilon$. Thus we employ symmetry and reduce the analysis of cluster states to the dynamics of the corresponding quotient network [29].

In a second step we derive conditions under which an avalanche of a certain size will indeed not decay into smaller groups.

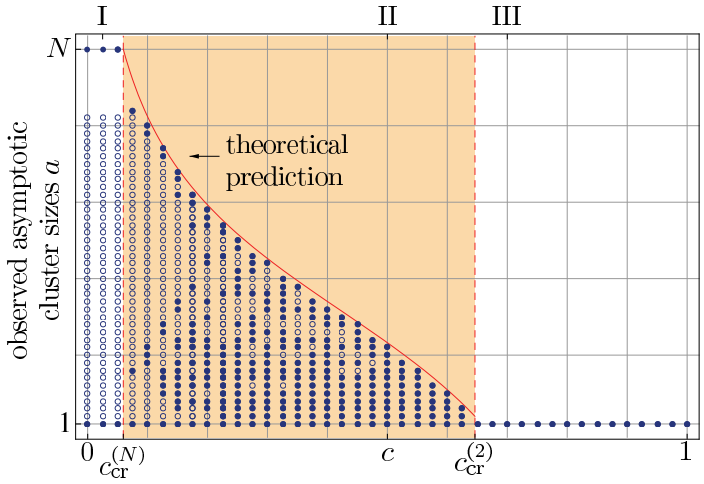

FIG. 3.2. *Sequential desynchronization transition in a network of $N = 50$ units ($U = U_b$, $b = -3$, $\tilde{\varepsilon} = 0.0175$). Cluster sizes a observed in the asymptotic network dynamics of 500 simulations for each $c \in \{0, 0.025, \ldots, 1\}$ starting from a perturbed synchronous state (•; cf. Figure 3.1) or from random phases distributed uniformly in $[0, 1)$ (∘). The shaded area marks the sequential desynchronizing transition, and the solid line shows the exact theoretical prediction (3.32) continuously interpolating the $N - 1$ bifurcation points $c_{\mathrm{cr}}^{(a)}$, $a \in \{2, 3, \ldots, N\}$, above which clusters of size a become unstable. The gap for cluster sizes $43 < a < 50$ at $0 < c < c_{\mathrm{cr}}^{(2)}$ appears, as cluster states involving these avalanche sizes do not exist according to Lemma 3.3.*

3.3. Notation: State space, firing, and return map. A state of a network of N pulse-coupled oscillators is completely specified by a phase vector

$$\Phi = (\phi_1, \phi_2, \ldots, \phi_N) \in S^N = \underbrace{S^1 \times \cdots \times S^1}_{N \text{ times}}, \tag{3.4}$$

where $\phi_i \in S^1 = \mathbb{R}/\mathbb{Z}$ are the phases of the individual units. Since the time evolution in between avalanches is a pure phase shift (2.14), it is convenient to consider a Poincaré section $\mathcal{S}$ of S^N with states just before the firing of one or more oscillators, i.e.,

$$\mathcal{S} = \left\{\Phi \in S^N \mid \exists j \in \{1, \ldots, N\}\,,\ \phi_j = 1\right\}. \tag{3.5}$$

It is convenient to relabel the oscillators after each avalanche such that $1 = \phi_1 \geq \phi_2 \geq \cdots \geq \phi_{N-1} \geq \phi_N > 0$. To specify the state of the network completely, we recall the permutation π^{-1} used for relabeling of the oscillators. The largest phase $\phi_1 = 1$ thus belongs to the oscillator $i = \pi(1)$, the second largest ϕ_2 to $i = \pi(2)$, etc. Thus an equivalent description of the state space $\mathcal{S}$ is given by

$$\mathcal{S}^p = \left\{\left((\phi_2, \ldots, \phi_N)\,, \pi\right) \in S^{N-1} \times S_N \mid 1 \geq \phi_2 \geq \cdots \geq \phi_{N-1} \geq \phi_N \geq 0\right\}. \tag{3.6}$$

Here S_N is the group of all permutations of N elements. We use the convention that all index labels i are taken modulo the network size N, e.g., labels i and $i + N$ denote the same oscillator.

The Poincaré map of the network dynamics for the Poincaré section $\mathcal{S}$ is the *firing map* $\mathbf{K}$ that maps the state $\Phi \in \mathcal{S}$ of the network just before the sth firing time t_s of an avalanche to the state just before the next avalanche that occurs at time t_{s+1}:

$$\mathbf{K}\left(\Phi\left(t_s^-\right)\right) = \Phi\left(t_{s+1}^-\right) \in \mathcal{S}. \tag{3.7}$$

Having determined the next avalanche Θ from a state $\Phi \in \mathcal{S}$, the map $\mathbf{K}$ is a composition of the avalanche map (2.17) and a subsequent shift of all phases to a state in $\mathcal{S}$. Note that the firing map is fully determined by the pair (Θ, σ), which is a function of Φ. We denote a phase shift of size σ by

$$S(\phi, \sigma) := S_\sigma(\phi) := \phi + \sigma. \tag{3.8}$$

The equivalent firing map acting on the state space $\mathcal{S}^p$ is denoted by $\mathbf{K}^p$. For the phase part we write

$$\mathbf{K}^p_\Phi\left(\left(\psi_2^{(0)}, \ldots, \psi_N^{(0)}\right), \pi^{(0)}\right) = \left(\psi_2^{(1)}, \ldots, \psi_N^{(1)}\right).$$

To track the network dynamics we consider a mapping of the state just before a fixed reference oscillator k fires in an avalanche at time t_r to the state just before this oscillator fires again at t_{r+1}:

$$\mathbf{M}\left(\Phi\left(t_r^-\right)\right) = \Phi\left(t_{r+1}^-\right). \tag{3.9}$$

$\mathbf{M}$ is called the *return map* and is the Poincaré map of the system on the section $\{\Phi \in \mathcal{S} \mid \phi_k = 1\}$. Again the equivalent return map acting on $\mathcal{S}^p$ is denoted by $\mathbf{M}^p$. The number m of avalanches occurring in the application of the return map is a function of the initial phase vector $\Phi = \Phi(t_r^-)$ and thus the return map $\mathbf{M}$ is a composition of m firing maps $\mathbf{K}$. Hence $\mathbf{M}$ is completely specified by an ordered *firing sequence*

$$\mathcal{F} = \mathcal{F}(\Phi) = \{(\Theta_s, \sigma_s)\}_{s=1}^m, \tag{3.10}$$

where the pairs (Θ_s, σ_s) specify the avalanche set Θ_s and subsequent shift σ_s of the sth firing map.

Given a firing sequence (3.10), we set $a_s = |\Theta_s|$ and, in the case of homogeneous networks with coupling (3.1), $\varepsilon_s = a_s\varepsilon$. A composition of shift and interaction maps is denoted as

$$\bigodot_{s=1}^{m} (S_{\sigma_s} \circ H_{\varepsilon_s})(\phi) := S_{\sigma_m} \circ H_{\varepsilon_m} \circ S_{\sigma_{m-1}} \circ H_{\varepsilon_{m-1}} \circ \cdots \circ S_{\sigma_2} \circ H_{\varepsilon_2} \circ S_{\sigma_1} \circ H_{\varepsilon_1}(\phi). \tag{3.11}$$

3.4. Existence and stability of asynchronous periodic states in meta-oscillator networks.

DEFINITION 3.1. *An* asynchronous periodic state *of a network of N pulse-coupled oscillators is a state $\Phi \in \mathcal{S}$ which is invariant under the return map, i.e., $\mathbf{M}(\Phi) = \Phi$, and with avalanche sizes $a_s = 1$, $s \in \{1, 2, \ldots, N\}$, i.e., each oscillator generates a pulse separately.*

Initially assume that all clusters stay forward invariant, i.e., do not decay into smaller subclusters during the network dynamics (cf. section 3.2), and thus consider networks of meta-oscillators with effective coupling matrix (3.3). A periodic cluster state in the original model thus becomes a periodic asynchronous state in the reduced effective meta-network. In the following we derive conditions for the existence of the asynchronous state and its stability in a meta-network.

LEMMA 3.2. *Consider a network* (2.14)–(2.17) *of N oscillators with pulse coupling matrix* (3.3) *and neuronal partial reset. Let $\Sigma = (\sigma_1, \ldots, \sigma_N) \in \mathbb{R}^N$ and define $\mathbf{L} : \mathbb{R}^N \times S^1 \to \mathbb{R}^N$ by*

$$\mathbf{L}_i(\Sigma, \phi) := \bigodot_{s=i+1}^{N+i-1} (S_{\sigma_s} \circ H_{\varepsilon_s}) \circ S_{\sigma_i} \circ J_{\varepsilon_{ii}}(\phi)$$

for $i \in \{1, 2, \ldots, N\}$. Then the asynchronous state exists if and only if there is a solution $\Sigma^* \in \mathbb{R}^N$ to the equation

$$\mathbf{L}(\Sigma, 1) = (1, 1, \ldots, 1) \tag{3.12}$$

that satisfies $\sigma_r^* > 0$ for all $r \in \{1, 2, \ldots, N\}$.

Proof. Assume there is a solution Σ^*, $\sigma_i^* > 0$. Set

$$\phi_1^* = 1, \qquad \phi_i^* = \left(H_{\varepsilon_1}^{-1} \circ S_{\sigma_1^*}^{-1}\right) \circ \left(H_{\varepsilon_2}^{-1} \circ S_{\sigma_2^*}^{-1}\right) \circ \cdots \circ \left(H_{\varepsilon_{i-1}}^{-1} \circ S_{\sigma_{i-1}^*}^{-1}\right)(1)$$

for $i \in \{2, \ldots, N\}$. Using that Σ^* is a solution to (3.12), we have $\bigodot_{r=1}^{N-1} \left(S_{\sigma_r^*} \circ H_{\varepsilon_r}\right) \circ S_{\sigma_N^*} \circ J_{\varepsilon_{NN}}(1) = 1$ and $\phi_N^* = S_{\sigma_N^*} \circ J_{\varepsilon_{NN}}(1) > 0$ since $\sigma_N^* > 0$. Further using $\varepsilon_i > 0$ and $\sigma_r^* > 0$, the phases are ordered according to $\phi_1^* = 1 > \phi_2^* > \cdots > \phi_N^* > 0$ and $\Phi^* = (\phi_1^*, \phi_2^*, \ldots, \phi_N^*) \in \mathcal{S}$.

Starting from the state Φ^*, the first pulse of oscillator $i = 1$ results in potentials $u_1^{(1)} = R(\varepsilon_{11})$, $u_i^{(1)} = U(\phi_i^*) + \varepsilon_1$, $i \in \{2, 3, \ldots, N\}$. Since $R(\varepsilon_{ii}) \leq \varepsilon_{ii} \leq \varepsilon_i < \varepsilon_i + U(\phi)$ for all $\phi > 0$ and $H_{\varepsilon_i}(\phi) < H_{\varepsilon_i}(\psi)$ for $\phi < \psi$, we have $u_1^{(1)} < u_N^{(1)} < u_{N-1}^{(1)} < \cdots < u_2^{(1)}$. Further

$$u_2^{(1)} = U(\phi_2^*) + \varepsilon_1 = U\left(\left(H_{\varepsilon_1}^{-1} \circ S_{\sigma_1^*}^{-1}\right)(1)\right) + \varepsilon_1 = U(1 - \sigma_1^*) < 1$$

as $\sigma_1^* > 0$. Thus oscillator $i = 1$ fires without triggering any further oscillators, yielding an avalanche set $\Theta_1 = \{1\}$. In addition the oscillators have to be shifted by σ_1^* to obtain $\phi_2 = 1$. Thus the first pair in the firing sequence is $(\{1\}, \sigma_1^*)$. Applying the same arguments to the new phases $\Phi^{*(1)} = \mathbf{K}(\Phi^*)$ yields $(\{2\}, \sigma_2^*)$ for the second pair. Repeating these steps N times, one obtains a firing sequence

$$\mathcal{F}(\Phi^*) = \{(\{r\}, \sigma_r^*)\}_{r=1}^N.$$

Thus

$$\begin{aligned}
\mathbf{M}_i(\Phi^*) &= \bigodot_{r=i+1}^{N} \left(S_{\sigma_r^*} \circ H_{\varepsilon_r}\right) \circ S_{\sigma_i^*} J_{\varepsilon_{ii}} \circ \bigodot_{r=1}^{i-1} \left(S_{\sigma_r^*} \circ H_{\varepsilon_r}\right)(\phi_i^*) \\
&= \bigodot_{r=i+1}^{N} \left(S_{\sigma_r^*} \circ H_{\varepsilon_r}\right) \circ S_{\sigma_i^*} J_{\varepsilon_{ii}}(1) \\
&= \left(H_{\varepsilon_1}^{-1} \circ S_{\sigma_1^*}^{-1}\right) \circ \left(H_{\varepsilon_2}^{-1} \circ S_{\sigma_2^*}^{-1}\right) \circ \cdots \circ \left(H_{\varepsilon_{i-1}}^{-1} \circ S_{\sigma_{i-1}^*}^{-1}\right)(1) \\
&= \phi_i^*,
\end{aligned}$$

using (3.12) in the third row. Hence $\mathbf{M}(\Phi^*) = \Phi^*$ and the asynchronous state Φ^* is invariant under the return map.

Conversely, a periodic asynchronous state yields a solution to (3.12), since each oscillator fires separately, and thus there is a phase shift $\sigma_i > 0$ after each pulse generation of the oscillators $i \in \{1, 2, \ldots, N\}$. Invariance of the periodic asynchronous state then shows that in fact $\Sigma = (\sigma_1, \sigma_2, \ldots, \sigma_N)$ is a solution to (3.12). Hence there is no periodic asynchronous state if the solution does not exist. If there is a solution with $\sigma_i^* \leq 0$, let s be the smallest index such that $\sigma_s^* \leq 0$. Starting in the state Φ^*

the first firing of oscillator $i = s$ will cause oscillator $i = s + 1$ to fire in the same avalanche since its potential at this point is given by

$$u_{s+1}^{(1)} = U\left[\bigodot_{r=1}^{s-1}\left(S_{\sigma_r^*}\circ H_{\varepsilon_r}\right)\left(\phi_{s+1}^*\right)\right] + \varepsilon_s$$
$$= U\left[H_{\varepsilon_s}^{-1}\circ S_{\sigma_s^*}^{-1}(1)\right] + \varepsilon_s = U\left(1-\sigma_s^*\right) \geq 1,$$

i.e., $\{s, s+1\} \subset \Theta_s$ and the system is not in a periodic asynchronous state. ∎

COROLLARY 3.3. *In a network* (2.14)–(2.17) *of N oscillators with homogeneous all-to-all coupling matrix* (3.1)*, an asynchronous (splay) state exists.*

Proof. Let

$$L(\sigma) := \bigodot_{s=1}^{N-1}\left(S_\sigma\circ H_\varepsilon\right)\circ S_\sigma\circ J_0(1).$$

Now since $L(0) = U^{-1}(\varepsilon(N-1)) < 1$ and $\frac{\partial}{\partial\sigma}L(\sigma) \geq 1$ the intermediate value theorem ensures the existence of a $\sigma^* > 0$ satisfying $L(\sigma^*) = 1$. $\Sigma^* = (\sigma^*, \ldots, \sigma^*)$ is a solution to (3.12). As $\varepsilon_{ii} = 0$, no oscillator receives suprathreshold input in the asynchronous state, i.e., $\zeta = 0$, and this result is independent of the partial reset function R as $R(0) = 0$ (cf. Definition 2.1). ∎

In Figure 3.2 we observe no cluster states involving avalanches of sizes 43 to 49. This is precisely because (3.12) has no solutions when setting $\varepsilon_i = a_i\varepsilon$, $\varepsilon_{ii} = (a_i - 1)\varepsilon$ for $a_1 \in \{43, 44, \ldots, 49\}$ and any further $0 < a_i \in \mathbb{N}$, $i \geq 1$, and m such that $\sum_{s=1}^m a_s = 50$.

Note that Lemma 3.2 holds for any rise function U. If there are q different positive solutions to (3.12), there coexist q different periodic asynchronous states. A convex U ensures that the solution is unique because $\mathbf{L}(\Sigma, 1)$ then becomes invertible for all $\Sigma \in \mathbb{R}^N$. Another consequence of convexity is that given the existence of an asynchronous state in a meta-oscillator network it is linearly stable, as the following theorem shows.

THEOREM 3.4. *Consider a network* (2.14)–(2.17) *of N oscillators with pulse coupling matrix* (3.3) *and neuronal partial reset. If a periodic asynchronous state exists, it is linearly stable.*

Proof. Existence of the asynchronous state $(\Phi^*, \mathrm{id}) \in \mathcal{S}^p$ with $\Phi^* = (\phi_2^*, \ldots, \phi_N^*)$ implies invariance under the return map $\mathbf{M}^p$,

$$\mathbf{M}^p(\Phi^*, \mathrm{id}) = (\Phi^*, \mathrm{id}). \tag{3.13}$$

For the intermediate states we set

$$\left(\Phi^{(s)}, \pi^{(s)}\right) := \left(\mathbf{K}^p\right)^s(\Phi^*, \mathrm{id}), \quad s \in \{0, 1, 2, \ldots, N\}.$$

If oscillator i generates a pulse, all oscillators $j \neq i$ receive the same input ε_i and oscillator i receives an input $\varepsilon_{ii} \leq \varepsilon_i$. Hence, using $R(\zeta) \leq \zeta$, we find that the oscillators do not change their firing order and $\pi^{(s)}$ is a cyclic permutation to the left $\pi^{(s)}(i) = i - s$.

To show that the asynchronous state is linearly stable, we add a small perturbation $\Delta^{(0)} = \left(\delta_1^{(0)}, \ldots, \delta_{N-1}^{(0)}\right)$ to the asynchronous state such that initially the phases are given by

$$\Psi^{(0)} := \left(\phi_1^{(0)}, \ldots, \phi_{N-1}^{(0)}\right) = \Phi^* + \Delta^{(0)}$$

and follow its time evolution. We neglect terms of $\mathcal{O}\big((\Delta^{(0)})^2\big)$ indicated by a dot above the equality sign ($\dot{=}$). We take the perturbation to be sufficiently small such that the oscillators still fire asynchronously, i.e., the avalanches are of size $a_s = 1$ and the order of the events is preserved. After s firing events the phases are

$$\Psi^{(s)} = \mathbf{K}_\Phi^p \left(\Psi^{(s-1)}, \pi^{(s-1)}\right) \dot{=} \mathbf{K}_\Phi^p \left(\Phi^{(s-1)}, \pi^{(r-1)}\right) + \Delta^{(s)} = \Phi^{(s)} + \Delta^{(s)},$$

where

$$\Delta^{(s)} = \mathbf{A}^{(s)} \Delta^{(s-1)}$$

is the phase perturbation before the next firing and $\mathbf{A}^{(s)}$ is the Jacobian matrix of $\mathbf{K}_\Phi^p$ at $\big(\Phi^{(s-1)}, \pi^{(s-1)}\big)$:

$$A_{ij}^{(s)} = \frac{d\mathbf{K}_i^p}{d\phi_j} \left(\Phi^{(s-1)}, \pi^{(s-1)}\right). \tag{3.14}$$

Setting $\sigma = 1 - H\left(\psi_2, \varepsilon_{\pi(1)}\right)$, the phase part of the firing map for $N \geq 3$ is

$$\boldsymbol{K}_\Phi^p (\Psi, \pi) = \begin{pmatrix} H\left(\psi_3, \varepsilon_{\pi(1)}\right) + \sigma \\ H\left(\psi_4, \varepsilon_{\pi(1)}\right) + \sigma \\ \dots \\ H\left(\psi_N, \varepsilon_{\pi(1)}\right) + \sigma \\ J\left(1, \varepsilon_{\pi(1)\pi(1)}\right) + \sigma \end{pmatrix}^T. \tag{3.15}$$

Inserting (3.15) into (3.14) gives

$$\mathbf{A}^{(s)} = \begin{pmatrix} -a_2^{(s)} & a_3^{(s)} & 0 & \dots & 0 \\ -a_2^{(s)} & 0 & a_4^{(s)} & \ddots & \vdots \\ \vdots & \vdots & \ddots & \ddots & 0 \\ -a_2^{(s)} & 0 & \dots & 0 & a_N^{(s)} \\ -a_2^{(s)} & 0 & \dots & 0 & 0 \end{pmatrix} \tag{3.16}$$

with

$$a_i^{(s)} = \frac{d}{d\phi} H_{\varepsilon_s}\left(\phi_i^{(s-1)}\right) = \frac{U'\left(\phi_i^{(s-1)}\right)}{U'\left(H_{\varepsilon_s}\left(\phi_i^{(s-1)}\right)\right)}. \tag{3.17}$$

Since $\varepsilon_j > 0$ it follows that $H_{\varepsilon_j}(\phi) = U^{-1}(U(\phi) + \varepsilon_j) > \phi$. Thus $a_i^{(s)} < 1$ since U is convex. Also $U' > 0$ and hence

$$0 < a_i^{(s)} < 1. \tag{3.18}$$

Now the Eneström–Kakeya theorem (cf. Appendix A and [25, 36, 4, 34]) applied to the matrix $\mathbf{A}^{(s)}$ shows that with these properties the spectral radius $\rho\left(\mathbf{A}^{(s)}\right)$ of $\mathbf{A}^{(s)}$ satisfies

$$\rho\left(\mathbf{A}^{(s)}\right) \leq r^{(s)} = \max_{i \in \{1,\dots,N-1\}} a_i^{(s)} < 1.$$

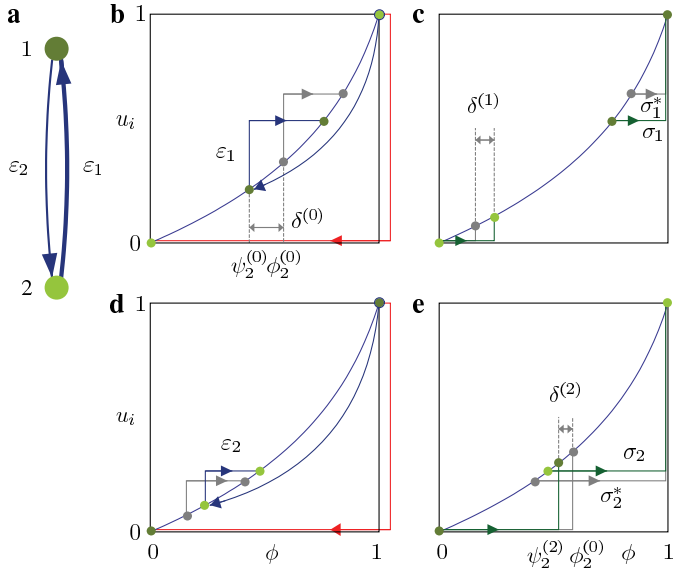

FIG. 3.3. *Stability of the asynchronous state (Theorem* 3.4*).* (a) *Graph of a network of* $N = 2$ *oscillators with connectivity* $\varepsilon_{ij} = (1 - \delta_{ij})\,\varepsilon_j$ *and* $0 < \varepsilon_2 < \varepsilon_1$. (b) *Firing of oscillator* $i = 1$. *For the oscillator* $i = 2$ *with initial phase* $\psi_2^{(0)} = \phi_2^{(0)} + \delta^{(0)}$ *smaller than in the invariant asynchronous state* $\phi_2^{(0)}$ *(gray), the input advances the phase* $\psi_2^{(0)}$ *more in comparison with the advance of* $\phi_2^{(0)}$ *in the asynchronous state due to the convexity of the rise function* U. (c) *After the interaction a subsequent shift completes the firing map* $\mathbf{K}$. *In total the derivation from the asynchronous state* $\delta^{(1)}$ *has become smaller.* (d) *Firing of oscillator* $i = 2$. *Phases which are perturbed to larger values than the asynchronous state are less advanced by inputs due to convexity of the rise function.* (d) *In total the return map* $\mathbf{M}$ *decreases the phase perturbations* $|\delta^{(2)}| < |\delta^{(0)}|$. *This stabilizing dynamics of the asynchronous state due to the convexity of the rise function generalizes to larger networks as proven in Theorem* 3.4.

Thus

$$\left\|\Delta^{(nN)}\right\| = \left\|\left(\prod_{r=1}^{N} \mathbf{A}^{(s)}\right)^n \Delta^{(0)}\right\| \le \prod_{r=1}^{N} \rho\left(\mathbf{A}^{(s)}\right)^n \left\|\Delta^{(0)}\right\| \to 0 \qquad \text{as } n \to \infty, \tag{3.19}$$

and the asynchronous state is linearly stable. For $N = 2$, $\rho\left(\mathbf{A}^{(s)}\right) = a_2 < 1$. ∎

This result is illustrated in Figure 3.3: Due to the convexity of the rise function, oscillators perturbed to larger (smaller) phases compared to the asynchronous state are less (more) advanced by input pulses pulling the perturbed phases back to the invariant asynchronous dynamics.

Combining Corollary 3.3 and Theorem 3.4 we obtain the following.

COROLLARY 3.5. *In a network* (2.14)–(2.17) *of* N *oscillators with homogeneous all-to-all coupling matrix* (3.1)*, neuronal partial reset* R*, and convex rise function* U*, the periodic asynchronous (splay) state exists and is linearly stable.*

3.5. Impact of partial reset on intracluster stability. In the state of synchronous firing, all units in an all-to-all coupled network receive a suprathreshold input pulse of strength $(N - 1)\,\varepsilon$, suggesting a rather strong influence of the partial reset R onto the network dynamics. Indeed, as shown in Figure 3.2, for the partial reset R_c one observes a sequential destabilization of clusters starting at large cluster sizes when increasing the reset strength c. In this subsection we study this behavior

analytically and explain the observed transition. The strategy is to focus on a single cluster of size a_1 and derive general conditions which ensure the stability of this cluster under the return map. As the return map depends on the firing sequence $\mathcal{F}$ we use best- and worst-case scenarios to obtain bounds for the stability of cluster states. We introduce a property of a rise function that allows us to estimate the worst- and best-case return maps by simpler return maps that do not depend on all details of the firing sequence $\mathcal{F}$. For a special class of rise functions, we find that a full analytical treatment is possible.

DEFINITION 3.6. *A firing sequence $\mathcal{F}$ is* admissible *if there is a state $\Phi \in \mathcal{S}$ which has firing sequence $\mathcal{F} = \mathcal{F}(\Phi)$. It is called* trigger invariant *if it is admissable and if for all oscillators $i \in \Theta_1^{(0)} = \{j \in \{1, 2, \ldots, N\} \mid \phi_j = 1\}$ triggering the first avalanche of the state $\Phi = (\phi_1, \ldots, \phi_N)$ (cf. (2.9)) the return map satisfies $\mathbf{M}_i(\Phi) = 1$. Thus for a trigger invariant firing sequence $\mathcal{F}$ with m intermediate avalanches $\Theta_1^{(0)} \subset \Theta_{m+1}^{(0)}$. The set of all trigger invariant firing sequences is denoted by $\mathcal{T}$. The subset of $\mathcal{F} \in \mathcal{T}$ with initial avalanche size $a_1 = |\Theta_1|$ is denoted by $\mathcal{T}_{a_1}$.*

Let us focus on a single avalanche of size a_1 in the network dynamics. To ensure that all units in this avalanche fire together again after the return map is applied, all units in this avalanche which were triggered to fire by $a \in \{1, 2, \ldots, a_1 - 1\}$ preceding spikes, i.e., with phases in

$$I_a^T = \left[U^{-1}(1 - a\varepsilon), 1\right],$$

have to be triggered again after applying the return map. Given a firing sequence $\mathcal{F} = \{(\varepsilon_r, \sigma_r)\}_{r=1}^m$ the return map for oscillators $i \in \Theta_1$ in the first avalanche is given by

$$M_{\mathcal{F}}(\phi) = \bigodot_{r=2}^{m} (S_{\sigma_r} \circ H_{\varepsilon_r}) \circ S_{\sigma_1} \circ J_{\varepsilon_1}(\phi).$$

Hence the conditions

$$\mathcal{M}_{\mathcal{F}}\left(I_a^T\right) \subset I_a^T \tag{3.20}$$

for all $a \in \{1, \ldots, a_1 - 1\}$ and all admissible firing sequences $\mathcal{F} \in \mathcal{T}_{a_1}$ ensure a cluster of size a_1 will not split up under return. By finding the most synchronizing and most desynchronizing firing sequences $\mathcal{F} \in \mathcal{T}_{a_1}$, i.e., the best- and worst-case scenarios, these conditions yield upper and lower bounds for the stability of a cluster of size a_1 under the return map.

LEMMA 3.7. *Consider a network* (2.14)–(2.17) *of N oscillators with homogeneous all-to-all coupling matrix* (3.1).

Set

$$w_a^{a_1} = \inf_{\mathcal{F} \in \mathcal{T}_{a_1}} M_{\mathcal{F}}\left(U^{-1}(1 - a\varepsilon)\right)$$

and

$$b_a^{a_1} = \sup_{\mathcal{F} \in \mathcal{T}_{a_1}} M_{\mathcal{F}}\left(U^{-1}(1 - a\varepsilon)\right).$$

Then the conditions

$$w_a^{a_1} \geq U^{-1}(1 - a\varepsilon) \tag{3.21}$$

for $a \in \{1, 2, \ldots, a_1 - 1\}$ *are sufficient and*

$$b_a^{a_1} \geq U^{-1}(1 - a\varepsilon) \tag{3.22}$$

are necessary for a cluster of size a_1 *to be invariant under return.*

Proof. $\frac{\partial}{\partial\phi} M_{\mathcal{F}}(\phi) > 0$, and thus conditions (3.20) are equivalent to

$$\mathcal{M}_{\mathcal{F}}\left(U^{-1}(1 - a\varepsilon)\right) \geq U^{-1}(1 - a\varepsilon) \tag{3.23}$$

for $a \in \{1, 2, \ldots, a_1 - 1\}$ and all admissible $\mathcal{F} \in \mathcal{T}_{a_1}$. ∎

Finding the $w_a^{a_1}$ and $b_a^{a_1}$ for general U and R can be done numerically using optimization techniques. However, there are two classes of rise functions (cf. Definition 3.8 and Lemma 3.9 below) which allow further analytical investigation as the effect of their worst- and best-case return maps can be estimated. Most of the commonly used rise functions, as, e.g., the rise function of the LIF neuron or the conductance-based LIF neuron, fall under one of these classes (cf. Appendix B).

The idea is to study the change of phase differences due to the application of the interaction function. Two oscillators initially at phases ϕ and $\phi + \Delta\phi$ receiving a pulse of strength ε will have a new phase difference

$$\Delta H(\phi, \Delta\phi, \varepsilon) := H_\varepsilon(\phi + \Delta\phi) - H_\varepsilon(\phi), \tag{3.24}$$

where the domain of ΔH is given by

$$\mathcal{D} := \left\{(\phi, \Delta\phi, \varepsilon) \mid 0 \leq \varepsilon \leq 1,\ 0 \leq \phi \leq 1,\ 0 \leq \Delta\phi \leq U^{-1}(1 - \varepsilon) - \phi\right\}.$$

Definition 3.8. *A rise function* U *is* increasing the change of phase differences (icpd) *if and only if*

$$\frac{\partial}{\partial\phi}\Delta H(\phi, \Delta\phi, \varepsilon) \geq 0 \quad \textit{for all } (\phi, \Delta\phi, \varepsilon) \in \mathcal{D}. \tag{3.25}$$

Conversely, it is decreasing the change of phase differences (dcpd) *if and only if*

$$\frac{\partial}{\partial\phi}\Delta H(\phi, \Delta\phi, \varepsilon) \leq 0 \quad \textit{for all } (\phi, \Delta\phi, \varepsilon) \in \mathcal{D}. \tag{3.26}$$

As shown in Appendix B.2 the icpd (dcpd) property is related to the third derivative of U. If the rise function is icpd or dcpd, the change in phase differences after application of the return map can be bounded as shown in the following lemma and illustrated in Figure 3.4(a)–(c) for icpd rise functions.

Lemma 3.9. *Let* ε_r, $\sigma_r \geq 0, r \in \{1, 2, \ldots, m\}$, $\varepsilon = \sum_{r=1}^m \varepsilon_r$, $\sigma_l \geq 0$. *Choose a* $\sigma_u \geq 0$ *such that*

$$\bigodot_{r=1}^{m} (S_{\sigma_r} \circ H_{\varepsilon_r})(\phi) \leq H_\varepsilon \circ S_{\sigma_u}(\phi)$$

and let $\phi \geq \psi$. *Then for an icpd rise function* U

$$\begin{aligned} S_{\sigma_l} \circ H_\varepsilon(\phi) - S_{\sigma_l} \circ H_\varepsilon(\psi) &\leq \bigodot_{r=1}^{m} (S_{\sigma_r} \circ H_{\varepsilon_r})(\phi) - \bigodot_{r=1}^{m} (S_{\sigma_r} \circ H_{\varepsilon_r})(\psi) \\ &\leq H_\varepsilon \circ S_{\sigma_u}(\phi) - H_\varepsilon \circ S_{\sigma_u}(\psi). \end{aligned} \tag{3.27}$$

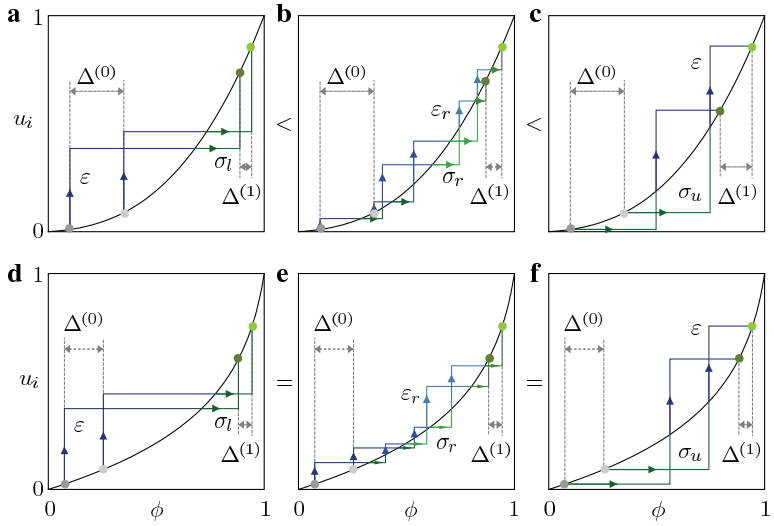

FIG. 3.4. *Rise functions with increasing change (icpd) and no change of phase differences.* (a)–(c) *Icpd rise function. An initial phase difference* $\Delta^{(0)}$ *changes to* $\Delta^{(1)}$ *after applying a combination of interaction maps* H_{ε_r} *(up arrows, colored blue in online version) of total strength* $\varepsilon = \sum_{r=1}^{m} \varepsilon_r$ *and shifts* S_{σ_r} *(right arrows, colored green in online version) such that the final maximal phase values are identical.* (a) *For icpd rise functions the difference* $\Delta^{(1)}$ *is the smallest when the interaction is applied in total before the shifts, i.e.,* $H_\varepsilon \circ S_{\sigma_l}$*, and* (c) *largest when applied after the shifts* $S_{\sigma_u} \circ H_\varepsilon$*.* (b) *All other maps* $\bigodot_{s=1}^{m} (H_{\varepsilon_s} \circ S_{\sigma_s})$ *produce phase differences which lie in between these extremal values (cf. Lemma* 3.9*).* (d)–(f) *The rise function* U_b *is icpd and dcpd, i.e., the phase difference* $\Delta^{(1)}$ *is independent of the order in which the interactions and shifts are applied.*

For U *that is dcpd,* (3.27) *holds replacing* $\leq$ *with* $\geq$*.*

Proof. Consider icpd rise functions first: To show the first inequality of (3.27) we use induction on m. The statement is clearly true for $m = 1$. Assume it is true for $m \geq 1$. Then

$$
\begin{aligned}
&S_{\sigma_l} \circ H_\varepsilon(\phi) - S_{\sigma_l} \circ H_\varepsilon(\psi) \\
&\quad = H_{\varepsilon_{m+1}} \circ H_{\varepsilon-\varepsilon_{m+1}}(\phi) - H_{\varepsilon_{m+1}} \circ H_{\varepsilon-\varepsilon_{m+1}}(\psi) \\
&\quad = \Delta H\left(H_{\varepsilon-\varepsilon_{m+1}}(\psi), H_{\varepsilon-\varepsilon_{m+1}}(\phi) - H_{\varepsilon-\varepsilon_{m+1}}(\psi), \varepsilon_{m+1}\right) \\
&\quad \leq \Delta H\left(H_{\varepsilon-\varepsilon_{m+1}}(\psi), \bigodot_{r=1}^{m} (S_{\sigma_r} \circ H_{\varepsilon_r})(\phi) - \bigodot_{r=1}^{m} (S_{\sigma_r} \circ H_{\varepsilon_r})(\psi), \varepsilon_{m+1}\right) \\
&\quad \leq \Delta H\left(\bigodot_{r=1}^{m} (S_{\sigma_r} \circ H_{\varepsilon_r})(\psi), \bigodot_{r=1}^{m} (S_{\sigma_r} \circ H_{\varepsilon_r})(\phi) - \bigodot_{r=1}^{m} (S_{\sigma_r} \circ H_{\varepsilon_r})(\psi), \varepsilon_{m+1}\right) \\
&\quad = \bigodot_{r=1}^{m+1} (S_{\sigma_r} \circ H_{\varepsilon_r})(\phi) - \bigodot_{r=1}^{m+1} (S_{\sigma_r} \circ H_{\varepsilon_r})(\psi),
\end{aligned}
$$

where we used the induction hypothesis and $\frac{\partial}{\partial \Delta\phi} \Delta H > 0$ (cf. (3.24)) in the third line, and in the fourth line the icpd property and the fact that $H_{\varepsilon-\varepsilon_{m+1}}(\psi) \leq \bigodot_{r=1}^{m} (S_{\sigma_r} \circ H_{\varepsilon_r})$ if $\sum_{r=1}^{m+1} \varepsilon_r = \varepsilon$, $\sigma_i \geq 0$. Substituting $\leq$ with $\geq$, we obtain the result for dcpd rise functions.

For the second inequality we also use induction over m. The statement is trivially

true for $m = 1$. Let it be true for $m \geq 1$ and let $\sigma_u \geq 0$ such that $\bigodot_{r=1}^{m+1} (S_{\sigma_r} \circ H_{\varepsilon_r})(\phi) \leq H_\varepsilon \circ S_{\sigma_u}(\phi)$. Then

$$\begin{aligned}
&H_\varepsilon \circ S_{\sigma_u}(\phi) - H_\varepsilon \circ S_{\sigma_u}(\psi) \\
&\quad = H_{\varepsilon_{m+1}} \circ H_{\varepsilon-\varepsilon_{m+1}} \circ S_{\sigma_u}(\phi) - H_{\varepsilon_{m+1}} \circ H_{\varepsilon-\varepsilon_{m+1}} \circ S_{\sigma_u}(\psi) \\
&\quad = \Delta H\left(H_{\varepsilon-\varepsilon_{m+1}} \circ S_{\sigma_u}(\psi), H_{\varepsilon-\varepsilon_{m+1}} \circ S_{\sigma_u}(\phi) - H_{\varepsilon-\varepsilon_{m+1}} \circ S_{\sigma_u}(\psi), \varepsilon_{m+1}\right) \\
&\quad \geq \Delta H\left(H_{\varepsilon-\varepsilon_{m+1}} \circ S_{\sigma_u}(\psi), \bigodot_{r=1}^{m} (S_{\sigma_r} \circ H_{\varepsilon_r})(\phi) - \bigodot_{r=1}^{m} (S_{\sigma_r} \circ H_{\varepsilon_r})(\psi), \varepsilon_{m+1}\right) \\
&\quad \geq \Delta H\left(\bigodot_{r=1}^{m} (S_{\sigma_r} \circ H_{\varepsilon_r})(\psi), \bigodot_{r=1}^{m} (S_{\sigma_r} \circ H_{\varepsilon_r})(\phi) - \bigodot_{r=1}^{m} (S_{\sigma_r} \circ H_{\varepsilon_r})(\psi), \varepsilon_{m+1}\right) \\
&\quad = \bigodot_{r=1}^{m+1} (S_{\sigma_r} \circ H_{\varepsilon_r})(\phi) - \bigodot_{r=1}^{m+1} (S_{\sigma_r} \circ H_{\varepsilon_r})(\psi),
\end{aligned}$$

where in the third line we used the implication

$$\bigodot_{s=1}^{m+1} (S_{\sigma_s} \circ H_{\varepsilon_s})(\phi) \leq H_\varepsilon \circ S_{\sigma_u}(\phi) \Rightarrow \bigodot_{s=1}^{m} (S_{\sigma_s} \circ H_{\varepsilon_s})(\phi) \leq H_{\varepsilon-\varepsilon_{m+1}} \circ S_{\sigma_u}(\phi) \tag{3.28}$$

to apply the induction hypothesis. In the fourth line we again used $\frac{\partial}{\partial \Delta\phi} \Delta H > 0$, (3.28), and the icpd property. Substituting $\geq$ with $\leq$, we obtain the result for dcpd rise functions. ∎

Using the previous result we can estimate the effect of worst- and best-case return maps on avalanches of a certain size and thus determine bounds on the network parameters which ensure invariance or decay of states that involve these cluster sizes.

THEOREM 3.10. *Consider a homogeneous excitatory all-to-all network of N pulse-coupled oscillators evolving according to* (2.14)–(2.17) *with neuronal partial reset R.*

For icpd rise functions U the conditions

$$\begin{aligned}
&U^{-1}(R((a_1-1)\varepsilon)) - U^{-1}(R((a_1-1)\varepsilon - a\varepsilon)) \\
&\qquad \leq U(1-(N-a_1)\varepsilon) - U^{-1}(1-(N-a_1)\varepsilon - a\varepsilon)
\end{aligned} \tag{3.29}$$

for all $a \in \{1, 2, \ldots, a_1 - 1\}$ are sufficient to ensure the invariance of an a_1-avalanche under return. Necessary conditions are

$$\begin{aligned}
&U^{-1}(R((a_1-1)\varepsilon) + (N-a_1)\varepsilon) - U^{-1}(R((a_1-1)\varepsilon - a\varepsilon) + (N-a_1)\varepsilon) \\
&\qquad \leq 1 - U^{-1}(1-a\varepsilon).
\end{aligned} \tag{3.30}$$

Likewise, for dcpd rise functions U, sufficient conditions are (3.30) *and necessary conditions* (3.29) *for an a_1-avalanche to not split up under return.*

Proof. Using Lemma 3.9 we find for an icpd rise function and $\mathcal{F} \in \mathcal{T}_{a_1}$

$$\begin{aligned}
&M_\mathcal{F}(1) - M_\mathcal{F}\left(U^{-1}(1-a\varepsilon)\right) \\
&\quad = \bigodot_{r=2}^{m} (S_{\sigma_r} \circ H_{\varepsilon_r})(S_{\sigma_1} \circ J_{\varepsilon_1}(1)) - \bigodot_{r=2}^{m} (S_{\sigma_r} \circ H_{\varepsilon_r})\left(S_{\sigma_1} \circ J_{\varepsilon_1}\left(U^{-1}(1-a\varepsilon)\right)\right) \\
&\quad \leq H_{(N-a_1)\varepsilon} \circ S_{\sigma_u} \circ J_{\varepsilon_1}(1) - H_{(N-a_1)\varepsilon} \circ S_{\sigma_u} \circ J_{\varepsilon_1}\left(U^{-1}(1-a\varepsilon)\right) \\
&\quad = 1 - H_{(N-a_1)\varepsilon} \circ S_\sigma \circ J_{\varepsilon_1}\left(U^{-1}(1-a\varepsilon)\right)
\end{aligned}$$

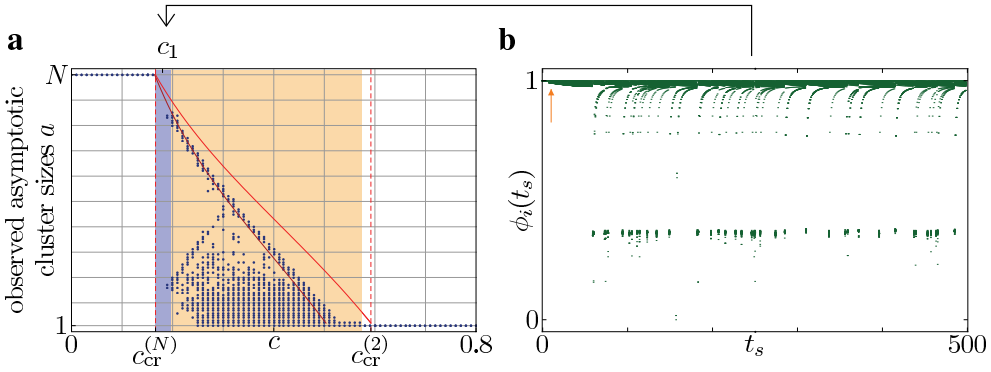

FIG. 3.5. *Sequential desynchronization in a network ($N = 100$) with icpd rise function $U_{\rm LIF}^{\rm CB}$ ($E_{\rm eq} = 1.1$, $E_{\rm syn} = 3$) and linear partial reset R_c.* (a) *Observed cluster sizes of periodic states after a time $t = 10000$. For each c value 100 simulations were started in the synchronous state with a small perturbation added. The upper line shows the bounds on a obtained from* (3.30) *in Theorem* 3.10*, above which a-clusters are unstable. The lower line is the bound obtained via* (3.29)*, below which a-clusters are ensured to be stable. The shaded area marks the transition region where states other than the synchronous and asynchronous state are observed. In the dark-shaded region (colored blue in the online version of this article) we find no periodic asymptotic dynamics. The dashed lines show the theoretical bounds for the transition region.* (b) *Aperiodic dynamics for $c_1 = 0.18$.*

with

$$\sigma_u = U^{-1}\left(1-(N-a_1)\,\varepsilon\right) - U^{-1}\left(R\,(a_1-1)\,\varepsilon\right), \tag{3.31}$$

and thus $w_a^{a_1} = H_{(N-a_1)\varepsilon} \circ S_{\sigma_u} \circ J_{\varepsilon_1}\left(U^{-1}\left(1-a\varepsilon\right)\right)$ in (3.21) yielding conditions (3.29). Similarly we find for (3.22), $b_a^{a_1} = 1 - H_{(N-a_1)\varepsilon} \circ J_{\varepsilon_1}(1) + H_{(N-a_1)\varepsilon} \circ J_{\varepsilon_1}\left(U^{-1}\left(1-a\varepsilon\right)\right)$, which yields the necessary conditions (3.30). For dcpd rise functions the expressions for $w_a^{a_1}$ and $b_a^{a_1}$ are interchanged. ∎

We used Theorem 3.4 to determine for a convex LIF rise function $U_{\rm LIF}^{\rm CB}$ (cf. (B.5) and (B.7)) and linear partial reset R_c the regime where avalanches of different sizes become unstable under return. The most strict condition in (3.29) is that for $a = 1$, which yields an implicit equation for the lower bounds on the critical c values below which the invariance of a_1-avalanches is ensured. The upper bound is obtained by (3.30) also using $a = 1$. Both bounds are plotted in Figure 3.5 and are in good agreement with the numerical data.

Near the lower transition point $c_{\rm crit}^{(N)}$ the system shows aperiodic behavior when starting close to the synchronous state. An explanation for this dynamics is the competition of two counteracting mechanisms: (i) Large avalanches become unstable under return and thus tend to desynchronize the phases, which results in a split of the avalanche into smaller stable avalanches. (ii) The solution to (3.12) for these asynchronously firing smaller clusters involves $\sigma_r^* \leq 0$; i.e., the smaller avalanches tend to absorb each other and resynchronize the system, yielding again larger unstable avalanches. Note that here irregular dynamics arise via a mechanism that differs from network heterogeneity [16] or using balanced excitatory and inhibitory interactions [71].

3.6. Extensive sequence of desynchronizing bifurcations—a solvable example. Figure 3.4(d)–(f) illustrates that the rise function U_b is both icpd and dcpd. In fact,

$$\Delta H_b\left(\phi, \Delta\phi, \varepsilon\right) := H_b\left(\phi + \Delta\phi, \varepsilon\right) - H_b\left(\phi, \varepsilon\right) = \Delta\phi e^{b\varepsilon}$$

is independent of ϕ and hence

$$\frac{\partial}{\partial\phi}\Delta H_b\left(\phi,\Delta\phi,\varepsilon\right)=0.$$

Thus for U_b equality holds in (3.27) and the best- and worst-case return maps become identical. This property allows us to obtain exact analytical results.

PROPOSITION 3.11. *Consider a homogeneous excitatory all-to-all network of N pulse-coupled oscillators evolving according to* (2.14)–(2.17) *with convex rise function U_b ($b<0$) and neuronal partial reset R_c.*

Then for each $2\le a\le N$ there exists a critical reset strength $c_{\mathrm{cr}}^{(a)}$ such that for all $c>c_{\mathrm{cr}}^{(a)}$ avalanches of size greater than or equal to a are unstable under return and avalanches of size smaller than a are stable. For $c\le c_{\mathrm{cr}}^{(N)}$ all avalanches are stable under return. The critical reset strengths are determined from the equation

$$e^{b\left(1-\left[(N-a)+c_{\mathrm{cr}}^{(a)}(a-1)\right]\varepsilon\right)}=\frac{\left(e^{-bc_{\mathrm{cr}}^{(a)}\varepsilon}-1\right)}{\left(e^{-b\varepsilon}-1\right)} \tag{3.32}$$

and satisfy $0<c_{\mathrm{cr}}^{(N)}<c_{\mathrm{cr}}^{(N-1)}<\cdots<c_{\mathrm{cr}}^{(2)}<1$.

Proof. Since U_b is icpd and dcpd, equality holds in (3.27), i.e., for $\mathcal{F}\in\mathcal{T}_{a_1}$

$$\Delta M_{\mathcal{F}}\left(\Delta\phi\right):=1-M_{\mathcal{F}}\left(1-\Delta\phi\right)=1-S_{\sigma_l}\circ H_{(N-a_1)\varepsilon}\circ J_{a_1\varepsilon}\left(1-\Delta\phi\right). \tag{3.33}$$

Thus the return map for the phase differences depends only on the avalanche size a_1 and is independent of the precise form of the other avalanches a_i, $i>1$, and intermediate shifts σ_i. Explicitly

$$\Delta M_{\mathcal{F}}\left(\Delta\phi\right)=\frac{e^{b\varepsilon(N-a_1+c(a_1-1))}}{1-e^b}\left(e^{-bc}\left(e^b+\left(1-e^b\right)\Delta\phi\right)^c-1\right)$$

for all $\mathcal{F}\in\mathcal{T}_{a_1}$. A straightforward calculation shows that $\Delta M_{\mathcal{F}}$ has the properties

$$\Delta M_{\mathcal{F}}\left(0\right)=0,\quad \frac{d}{d\Delta\phi}\Delta M_{\mathcal{F}}\left(\Delta\phi\right)\ge 0,\quad \text{and}\quad \frac{d^2}{d\Delta\phi^2}\Delta M_{\mathcal{F}}\left(\Delta\phi\right)\le 0. \tag{3.34}$$

Thus if the condition

$$\Delta M_{\mathcal{F}}\left(1-U^{-1}\left(1-\varepsilon\right)\right)\le 1-U^{-1}\left(1-\varepsilon\right) \tag{3.35}$$

is met, all other conditions for $1\le a<a_1$ in (3.29) are also satisfied. On the other hand almost all perturbations will cause the avalanche to be triggered by a single oscillator. Thus if condition (3.35) is not satisfied, i.e., $\Delta M_{\mathcal{F}}\left(\Delta\phi\right)>\Delta\phi$ for all $\Delta\phi\ge U^{-1}\left(1-\varepsilon\right)-1$, the avalanche will split up after a finite number of iterations of the return map. Thus (3.35) is a necessary and sufficient condition for stability of an a-cluster under the return map. We are interested in the critical strengths $c_{\mathrm{crit}}^{(a)}$ for which an a-cluster becomes unstable, and hence we use the equality in (3.35) and basic algebra to obtain the implicit expressions (3.32) for the $c_{\mathrm{cr}}^{(a)}$.

Since we have assumed $(N-1)\,\varepsilon<1$, $b<0$, and $c\in[0,1]$ we see that the left-hand side of (3.32) lies in the interval $(0,1)$ and decreases monotonically with increasing c. The right-hand side is 0 for $c=0$ and increases monotonically with c until it becomes 1 for $c=1$. Thus by continuity for all $2\le a\le N$ there always exists

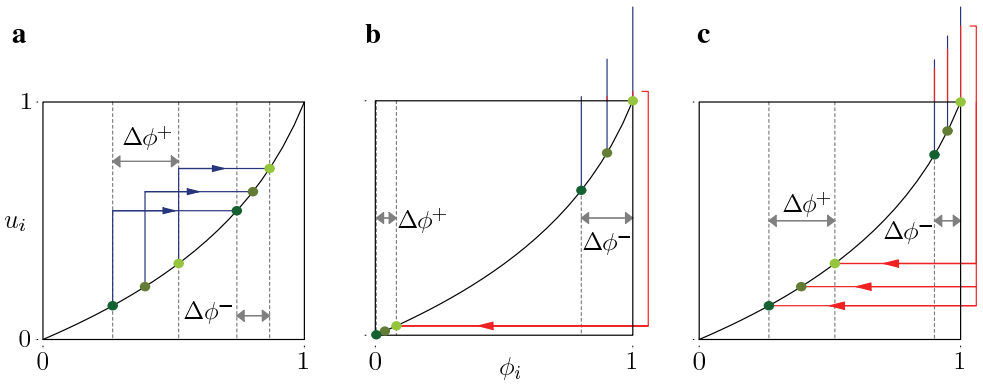

FIG. 3.6. *Synchronization and desynchronization of avalanches in networks with convex rise function and partial reset.* (a) *Subthreshold inputs synchronize the oscillators. The phase difference of a cluster before pulse reception $\Delta\phi^+$ is decreased to $\Delta\phi^-$ afterwards, i.e., $\Delta\phi^+ < \Delta\phi^-$.* (b) *Weak partial reset (e.g., $c \approx 0$ for R_c) synchronizes phase differences: $\Delta\phi^+ < \Delta\phi^-$.* (c) *Due to the convexity of the rise function a strong partial reset ($c \approx 1$) expands the phase differences $\Delta\phi^+ > \Delta\phi^-$. Clusters lose stability if the mechanism in* (c) *becomes dominant over the stabilizing effect* (a).

a solution $0 < c_{\mathrm{cr}}^{(a)} < 1$ to this equation. Note that the special case $a = 2$ is explicitly solvable for $c_{\mathrm{cr}}^{(2)}$ and yields

$$c_{\mathrm{cr}}^{(2)} = \frac{1}{b\varepsilon} \log\left(1 + e^{-b(N-2)\varepsilon + b}\left(1 - e^{-b\varepsilon}\right)\right). \tag{3.36}$$

For fixed $0 \le c < 1$ the left-hand side of (3.32) is strict monotonically decreasing as a increases, whereas the left-hand side is independent of a, and thus $0 < c_{\mathrm{cr}}^{(N)} < c_{\mathrm{cr}}^{(N-1)} < \cdots < c_{\mathrm{cr}}^{(2)} < 1$. □

The theoretical prediction (3.32) for the desynchronization transition is plotted in Figure 3.2 and is in excellent agreement with the numerically observed transition.

REMARK 3.12. *Note that* (3.32) *involves all relevant network parameters. In particular, choosing $b \to -\infty$ in* (3.36) *shows that $c_{\mathrm{cr}}^{(2)}$ can be made arbitrarily small. This implies that the entire sequence of desynchronizing bifurcations may occur over an arbitrary small interval $\left[c_{\mathrm{cr}}^{(N)}, c_{\mathrm{cr}}^{(2)}\right]$.*

REMARK 3.13. *We also remark that the number of bifurcation points in this sequence is $N - 1$. At each bifurcation point $c_{\mathrm{cr}}^{(a)}$ all periodic states with at least one cluster of size a and all other cluster sizes less than or equal to a, i.e., an extensive combinatorial number of states, become unstable simultaneously.*

The mechanisms underlying the desynchronization transition are opposing synchronization and desynchronization dynamics in the network, as illustrated in Figure 3.6: Due to the convexity of the rise function (a) subthreshold inputs are always synchronizing and stabilize the avalanche, whereas depending on the strength of the partial reset suprathreshold inputs in an avalanche can either (b) synchronize or (c) desynchronize the phases. Thus for a weak partial reset (e.g., R_c with $c \approx 0$) states with large avalanches are stable. When the partial reset is stronger it desynchronizes the cluster and, depending on the avalanche size, it may outweigh the synchronization effect due to subthreshold inputs. Larger avalanches receive less synchronizing subthreshold input from other oscillators and simultaneously produce a larger suprathreshold input than smaller ones. Thus they lose invariance under return first when increasing the partial reset strength.

4. Robustness of the desynchronization transition. The desynchronization transition is robust against structural perturbations in the coupling matrix and the rise function U.

4.1. Coupling strength inhomogeneity. With respect to perturbations in the coupling matrix ε_{ij}, numerical experiments show that the transition is observed when using coupling strengths from a uniform distribution on an interval $[\varepsilon_{\min}, \varepsilon_{\max}]$ for a interval length $\Delta\varepsilon = \varepsilon_{\max} - \varepsilon_{\min}$ as large as 20% of the average coupling strength $\bar{\varepsilon} = (\varepsilon_{\max} - \varepsilon_{\min})/2$. When $\Delta\varepsilon$ becomes larger, usually complex spike patterns and nonperiodic states are observed.

The coupling inhomogeneity destabilizes clusters since also subthreshold inputs of different strengths desynchronize units initially at the same phase. In fact, already the lower bound $c_{\mathrm{crit}}^{(a)}$ obtained for homogeneous networks via Theorem 3.10 using the coupling strength $\bar{\varepsilon}$ overestimates the stability of the clusters. The regime where we observe aperiodic dynamics becomes larger in comparison to homogeneous networks with the same average coupling strength. This is due to clusters with asymptotic phases which are close to an absorption (i.e., where $\sigma_i^* \approx 0$ for some i). A perturbation in the coupling now enables the absorption, and the restless competition between desynchronization and synchronization (cf. section 3.5) induces the aperiodic dynamics.

4.2. Sigmoidal rise functions. Typically rise functions in biological or physical systems are neither purely concave nor purely convex. In particular intrinsic neuronal dynamics is often best described with a sigmoidal rise function. The quadratic-integrate-and-fire or exponential-integrate-and-fire neuron [21, 24] (cf. also Appendix B) constitute major examples. In networks with sigmoidal rise functions a combination of the effects inherent to concave and convex rise functions influences the network dynamics: synchronization of units to larger clusters due to the concave part (cf. [48, 38]) and stabilization of states with asynchronously firing clusters due to the convex part (cf. Theorem 3.4). Numerical studies show that for strictly neuronal partial resets and rise functions with dominant concave part, synchronized firing of oscillators in the asymptotic state is typically found. In contrast, if the convex part is larger, it is more likely to find clusters of smaller sizes and the asynchronous state. Indeed, for general rise functions U we still obtain the stability matrix $\mathbf{A}$ in (3.16), but the nonzero entries (3.17) can become larger than 1 in the regime where U is concave. Thus if the concave part becomes dominant, the eigenvalues are no longer bounded by 1 and asynchronous cluster states become unstable.

In Figure 4.1 a desynchronization transition for the sigmoidal rise function $U_{\mathrm{QIF}}^{\mathrm{CB}}$ and linear partial reset R_c is shown. In the synchronous state oscillators do not receive any intermediate subthreshold pulses between successive firing, and the return map for an oscillator with phase ϕ can be written as

$$M_{\{\{1,\dots,N\},\sigma\}}(\phi) = U^{-1}\left(R\left(U(\phi) + (N-1)\varepsilon - 1\right)\right) + 1 - U^{-1}\left(R\left((N-1)\varepsilon\right)\right)$$

for any partial reset R and any rise function U. After a perturbation the avalanche is typically triggered by a single unit, and thus the synchronous state becomes unstable if $M_{\{\{1,\dots,N\},\sigma\}}(\phi) < \phi$ for all $\phi \in \left[1 - U^{-1}(1-\varepsilon), 1\right]$, which yields the condition (3.29) for $a_1 = N$. This can be used to determine the onset of a desynchronization transition in the general case, as shown in Figure 4.1 (dashed line). The stability of smaller avalanches $a_1 < N$ can still be estimated with the help of Theorem 3.10 if the rise function is dcpd but not necessarily convex. Conditions for the sigmoidal rise functions U_{QIF} and $U_{\mathrm{QIF}}^{\mathrm{CB}}$ to be dcpd are given in Appendix B.

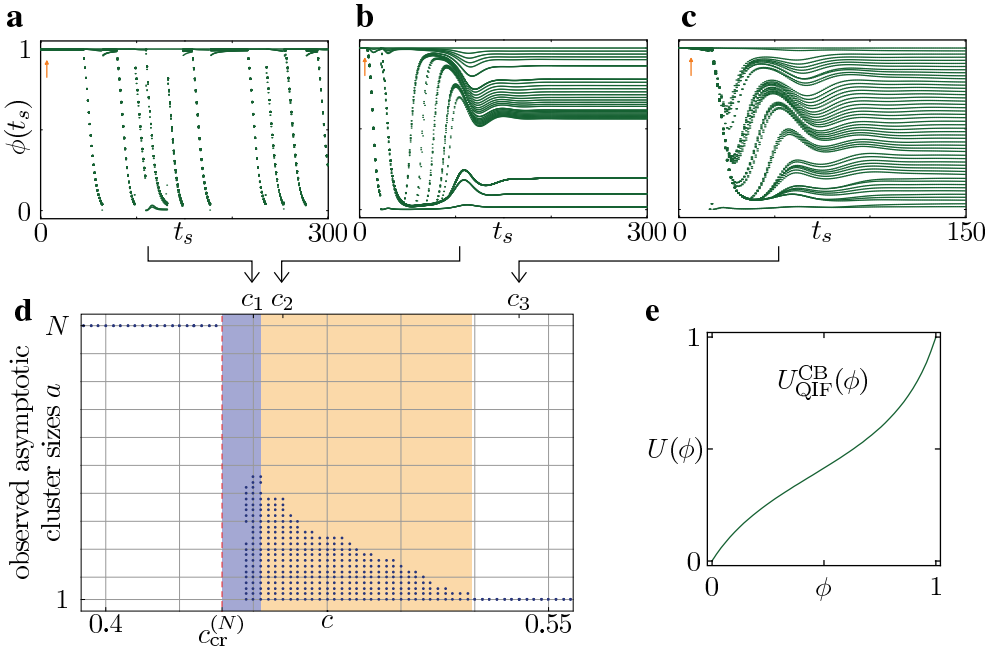

FIG. 4.1. *Sequential desynchronization transition in networks of neural oscillators with a sigmoidal rise function. Shown are the dynamics of a homogeneous network ($N = 100$, $\varepsilon = 0.002$) with linear partial reset R_c and* (e) *sigmoidal rise function $U_{\mathrm{LIF}}^{\mathrm{CB}}$ ($E_{\mathrm{syn}} = 2$, $\alpha = -1$, $\beta = 1$). Starting with synchrony and inducing a small perturbation (arrow) the network shows* (a) *aperiodic dynamics for $c = c_1 = 0.45$,* (b) *clustering for $c = c_2 = 0.46$, and* (c) *asynchronous dynamics for $c = c_3 = 0.54$. Note the oscillations of the phase which do not appear for purely convex rise functions (cf. Figure 3.5).* (d) *Cluster sizes of periodic states observed in the dynamics at $t = 5000$ starting from 200 perturbed synchronous states for each value of c. Shaded area marks the transition region with states other than solely synchronous or asynchronous. The dark-shaded region (colored blue in online version) marks the occurrence of aperiodic dynamics. The dashed line indicates critical $c_{\mathrm{crit}}^{(N)}$ determined from (3.23) for $a_1 = N$ above which synchronous firing becomes unstable.*

Desynchronization due to a partial reset has three components: Translation of phase differences into potential differences via the rise function U, the relative change of potential differences due to the partial reset R after suprathreshold excitation, and back-translation of this potential difference into phase differences via U^{-1} (cf. Figure 3.6(c)). For convex rise functions the slope in the reset zone $I^R = \left[0, U^{-1}\left(R\left((N-1)\varepsilon\right)\right)\right]$ is always smaller than in the suprathreshold zone $I^T = \left[U^{-1}\left(1-(N-1)\varepsilon\right), 1\right]$. As a consequence the phase differences in I^T are translated via U to larger potential differences, and the potential differences after reset become larger phase differences during the back translation U^{-1}. This causes an effective phase desynchronization even for partial resets that are nonexpansive, as depicted in Figure 3.6(c).

For general rise functions and nonexpansive partial resets, the destabilization of a cluster state due to a partial reset thus can occur only if the slopes in I^T are sufficiently larger than those in I^R. In fact if this ratio becomes too small, the transition may not be observed completely for nonexpansive partial reset, e.g., for R_c in the range $c \in [0, 1]$, and can be shifted to partial resets that have to be expansive (e.g., for $c > 1$).

Finally note that, in contrast to convex rise functions, for sigmoidal rise functions

we always observe "damped oscillations" in the Poincaré phase plots Figure 4.1(b,c). The amplitudes of these oscillations become larger when the slope of the rise function at the point of inflection becomes smaller. We therefore attribute these oscillations to subthreshold inputs received by oscillators near the inflection point of the rise function.

5. Discussion. In summary, we proposed a model of pulse-coupled threshold units with partial reset. This partial reset, an intrinsic response property of the local units, acts as a desynchronization mechanism in the collective network dynamics. It causes an extensive sequence of desynchronizing bifurcations of cluster state networks of pulse-coupled oscillators with convex rise function. This sequential desynchronization transition is robust against structural perturbations in the coupling strength and variations of the local subthreshold dynamics.

Previous studies have not particularly focused on the collective implications of partial or graded resets. In network models with pulses that are extended in time, typically a full conservation of the input is considered [68, 70, 30]. Models with instantaneous responses to inputs consider fully dissipative reset ($R(\zeta) \equiv 0$ in our model) [48, 27, 7, 59, 65, 64], fully conservative reset ($R(\zeta) = \zeta$) [9, 11], as well as both extremes [33] without discussing particular consequences of the reset mechanism. Here we closed this gap and showed that in fact the reset mechanism influences the synchronization processes.

Partial reset in pulse-coupled oscillators keeps the collective network dynamics analytically tractable and at the same time describes additional physically or biologically relevant dynamical features of local units. In neurons, for instance, synaptic inputs are collected in the dendrite and then transmitted to the cell body (soma). At the soma the integration of the membrane potential takes place and spikes are generated. Remaining input charges on the dendrite not used to trigger a spike at the soma may therefore contribute to the potential after somatic reset [17, 58, 10].

Such features are effectively modeled by the simple partial reset introduced here. In particular, spike time response curves (that may be obtained for any tonically firing neuron [51, 56, 50, 26]) encode the shortening of the interspike intervals (ISI) following an excitatory input at different phases of the neural oscillation. An excitatory stimulus that causes the neuron to spike will maximally shorten the ISI in which the stimulus is applied. Additionally, the second ISI that follows is typically affected as well, e.g., due to compartmental effects. It is exactly this shortening of the second ISI that is characterized by appropriately choosing a partial reset function in our simplified system. The details of such a description and consequences for networks of more complicated neuron models are studied separately [38]. For instance, networks of two-compartment conductance-based synaptically coupled neurons indeed exhibit similar desynchronization transitions when varying the coupling between soma and dendrite, which in our simplified model controls the partial reset.

The desynchronization due to the partial reset, i.e., due to local processing of suprathreshold input, differs strongly from that induced by previously known mechanisms based on, e.g., heterogeneity, noise, or delayed feedback [70, 69, 44, 40, 55, 16]. Possibly, this desynchronization mechanism may also be helpful in modified form to prevent synchronization in neural activity such as in Parkinson tremor or in epileptic seizures [63, 62].

In this work we developed a partial reset for suprathreshold inputs and considered purely homogeneous and globally excitatory instantaneously coupled systems. In networks with delayed excitatory interactions the full reset mechanism is responsible

for the collapse of state space volume to a lower dimension, explaining the occurrence of unstable attractors [5]. Changing to an invertible partial reset, the flow becomes locally invertible and the unstable attractors become saddle points with possible heteroclinic connections that entail switching dynamics (cf. [39]).

For inhibitory couplings one can define a lower threshold [15] below which inhibitory inputs become less effective, i.e., a partial inhibition. In models of neurons, for instance, this could characterize shunting inhibition [3]. If two units simultaneously receive inhibitory inputs below a lower threshold, a zero partial inhibition, i.e., setting the state of the units to a fixed lower value, is strongly synchronizing in analogy to a full reset after suprathreshold excitation. Our findings suggest that, similar to a partial reset, a less synchronizing nonzero partial inhibition may also have a strong influence on the collective network dynamics. Our partial reset model might also find applications in studying network dynamics of neurons with postinhibitory rebound [57]. These neurons get more excitable when hyperpolarized by inhibitory inputs, e.g., due to the opening of slowly inactivating calcium channels. After the release from sufficiently strong inhibition the neurons generate a spike and thereafter may still exhibit stronger excitability. In our simple model this enhanced excitability then could be modeled using a partial reset mechanism for inhibition.

In biologically more detailed neuronal network models, both excitatory and inhibitory couplings as well as complex network topologies play important roles in generating irregular [71] and synchronized spiking dynamics [2]. It would therefore be an interesting task to study the impact of partial resets in such networks.

Appendix A. The Eneström–Kakeya theorem.

A.1. Spectral-radius and matrix-norm. Let $\mathbf{A} = a_{ij}$ be an $n \times n$ matrix. The spectral radius ρ of an $\mathbf{A}$ is defined as [34]

$$\rho(\mathbf{A}) = \max_{\|\mathbf{x}\|=1} \|\mathbf{A}\mathbf{x}\| = \max_{i=1,\dots,n} |\lambda_i|\,, \tag{A.1}$$

where $\|\|$ denotes a norm and $\{\lambda_i\}_{i=1}^n$ are the complex eigenvalues of $\mathbf{A}$. If $\|-\|$ is any matrix norm (see [46]), the inequality

$$\rho(A) \le \|A\| \tag{A.2}$$

is valid and in fact $\rho(A) = \inf \|A\|$, where the infimum is taken over all matrix norms [34]. Here we only need the *maximum-absolute-column-sum norm* of $\mathbf{A}$ defined as

$$\|\mathbf{A}\| = \max_{j=1,\dots,n} \sum_{i=1}^{n} |a_{ij}|\,. \tag{A.3}$$

A.2. Companion matrices. An $(n+1) \times (n+1)$ companion matrix $\mathbf{C}$ has the standard form

$$\mathbf{C} = \begin{pmatrix} 0 & \dots & 0 & -\tilde{c}_0 \\ 1 & & 0 & -\tilde{c}_1 \\ & \ddots & & \vdots \\ 0 & & 1 & -\tilde{c}_n \end{pmatrix} \tag{A.4}$$

with characteristic polynomial

$$\tilde{p}_{n+1}(z) = \det(z - \mathbf{C}) = \tilde{c}_0 + \tilde{c}_1 z + \cdots + \tilde{c}_n z^n + z^{n+1}. \tag{A.5}$$

A.3. The Eneström–Kakeya theorem. The Eneström–Kakeya theorem[1] [25, 36, 35, 4, 34] can be stated in the following form.

THEOREM A.1. *Let* $p_n(z) = \sum_{j=0}^{n} c_j z^j$ *with* $c_j > 0$*; then for all* λ *with* $p_n(\lambda) = 0$

$$|\lambda| \leq \max_{0 \leq i < n} \left\{ \frac{c_i}{c_{i+1}} \right\} =: \beta.$$

Proof. Note first that $\beta > 0$. We set

$$\tilde{p}_{n+1}(z) := \frac{(z-1)p_n(\beta z)}{c_n \beta^n} = z^{n+1} + \sum_{i=0}^{n} \tilde{c}_i z^i, \tag{A.6}$$

where

$$\tilde{c}_i = \begin{cases} \frac{c_{i-1} - \beta c_i}{c_n \beta^{n-i+1}}, & 1 \leq i \leq n, \\ \frac{-c_0}{c_n \beta^n}, & i = 0. \end{cases}$$

Using the definition of β one observes that $\tilde{c}_j \leq 0$. Comparing (A.5) with (A.6) the companion matrix of $\tilde{p}_{n+1}$ is given by (A.4). Since $1 + \sum_{j=1}^{n+1} \tilde{c}_j = \tilde{p}_{n+1}(1) = 0$ it follows that $\|\mathbf{C}\| = \sum_{j=1}^{n+1} |\tilde{c}_j| = -\sum_{j=1}^{n+1} \tilde{c}_j = 1$ when using the maximum-absolute-column-sum norm (A.3), and hence from (A.2)

$$\rho(\mathbf{C}) \leq 1.$$

Thus for all $\tilde{\lambda}$ with $p_{n+1}(\tilde{\lambda}) = 0$ we have $|\tilde{\lambda}| \leq \rho(\mathbf{C}) \leq 1$. For a λ with $p_n(\lambda) = 0$ it follows from the definition of $\tilde{p}_{n+1}$ that $\tilde{p}_{n+1}(\tilde{\lambda}) = 0$ for $\tilde{\lambda} = \frac{\lambda}{\beta}$ and thus $|\lambda| \leq \beta$. ∎

COROLLARY A.2. *Let* $\mathbf{A}$ *be a matrix of the form (cf.* (3.16)*)*

$$\mathbf{A} = \begin{pmatrix} -a_n & a_1 & 0 & \dots & 0 \\ -a_n & 0 & a_2 & \ddots & \vdots \\ \vdots & \vdots & \ddots & \ddots & 0 \\ -a_n & 0 & \dots & 0 & a_{n-1} \\ -a_n & 0 & \dots & 0 & 0 \end{pmatrix}$$

with $a_i > 0$*; then*

$$\rho(\mathbf{A}) \leq \max \{a_i\}_{i=1}^{n}.$$

Proof. By a permutation of rows and columns we can cast $\mathbf{A}$ into a matrix $\mathbf{B} = b_{i,j}$ with nonzero entries $b_{i,(i+1)} = a_i$, $i \in \{1, \dots, n-1\}$, and $b_{i,n} = -a_n$, $i \in \{1, \dots, n\}$. This does not change the spectral radius. The similarity transformation to $\mathbf{C} = \mathbf{Q}^{-1}\mathbf{B}\mathbf{Q}$ with $\mathbf{Q} = \operatorname{diag}(q_1, \dots, q_{N-1})$ and $q_1 = 1$, $q_i = \prod_{j=1}^{i-1} a_j$, $i \in \{2, \dots, n\}$, also preserves the spectral radius, and $\mathbf{C}$ has the form of a companion matrix (A.4) with $c_i = \prod_{j=i+1}^{n} a_i > 0$, $i \in \{0, \dots, n-1\}$. Thus $\rho(\mathbf{A}) = \rho(\mathbf{C}) \leq \max_{0 \leq i < n} \left\{ \frac{c_i}{c_{i+1}} \right\} = \max_{1 \leq i \leq n} \{a_i\}$. ∎

[1] In 1893 the Swedish actuary and mathematics historian Gustaf Eneström published this result of roots of certain polynomials with real coefficients in a paper on pension insurance (in Swedish) [25]. This result is now often called the Eneström–Kakeya theorem, since S. Kakeya published a similar result in 1912–1913 [36]. But Kakeya's theorem contained a mistake, which was corrected by A. Hurwitz in 1913 [35].

Appendix B. Rise functions.

B.1. Rise functions for integrate-and-fire models. In this section we derive the rise functions for single variable models of the form

$$\frac{d}{dt}v = F(v) + I_{\text{in}}(t).$$

We distinguish between potential independent inputs $I_{\text{in}}(t) = P(t)$ with $P(t) = \sum_s \varepsilon_s \delta(t - t_s)$ and the conductance-based approach $I_{\text{in}}(t) = g_{\text{syn}} P(t)(E_{\text{syn}} - v(t))$, $E_{\text{syn}} > 1$. More generally, if $I_{\text{in}}(t) = Q(v(t))P(t)$ and $Q(t) > 0$, the transformation

$$u(t) = \frac{1}{M}\int_0^{v(t)} \frac{1}{Q(v)}\mathrm{d}v, \qquad M = \int_0^1 \frac{1}{Q(v)}\mathrm{d}v \tag{B.1}$$

yields

$$\frac{d}{dt}u = \hat{F}(u) + \frac{1}{M}P(t), \qquad \hat{F}(u) = \frac{1}{M}\frac{F(v(u))}{Q(v(u))}, \tag{B.2}$$

i.e., a potential independent input I_{in}. Thus if the rise function U for $I_{\text{in}}(t) = P(t)$ is known, the conductance-based rise function U^{CB} is calculated with the help of (2.13) as

$$U^{\text{CB}}(\phi) = \frac{\ln\left(1 - E_{\text{syn}}^{-1} U(\phi)\right)}{\ln\left(1 - E_{\text{syn}}^{-1}\right)}. \tag{B.3}$$

The leaky-integrate-and-fire (LIF) model [42] is given by $F(u) = -g_l u + I_{\text{ext}}$, which yields

$$U_{\text{LIF}}(\phi) = E_{\text{eq}}\left(1 - e^{-g_l T_{\text{LIF}}\phi}\right), \tag{B.4}$$

where $T_{\text{LIF}} = -\frac{1}{g_l}\ln(1 - E_{\text{eq}})$ and $E_{\text{eq}} = \frac{I_{\text{ext}}}{g_l} + E_l > 1$. This yields

$$U_{\text{LIF}}^{\text{CB}}(\phi) = \frac{\ln\left(1 - E_{\text{syn}}^{-1} U_{\text{LIF}}(\phi)\right)}{\ln\left(1 - E_{\text{syn}}^{-1}\right)}. \tag{B.5}$$

For the quadratic-integrate-and-fire (QIF) model [24] with $F(u) = g_2(E_r - u)(E_t - u) + I_{\text{ext}}$, one obtains for $I_{\text{syn}}(t) = P(t)$

$$U_{\text{QIF}}(\phi) = \frac{\alpha - \tan\left(\arctan(\alpha) - \phi\left(\arctan(\alpha) - \arctan(\beta)\right)\right)}{\alpha - \beta}, \tag{B.6}$$

where $\alpha = \frac{E_r + E_t}{\gamma}$, $\beta = \alpha - \frac{2}{\gamma}$, $\gamma = \sqrt{\frac{4I_{\text{ext}}}{g_2} - (E_t - E_r)^2} > 0$. Hence

$$U_{\text{QIF}}^{\text{CB}}(\phi) = \frac{\ln\left(1 - E_{\text{syn}}^{-1} U_{\text{QIF}}(\phi)\right)}{\ln\left(1 - E_{\text{syn}}^{-1}\right)}. \tag{B.7}$$

Note that depending on the integrate-and-fire model and coupling type, convex, concave, and sigmoidal shapes are possible (cf. Table B.1). We remark that as $E_{\text{syn}} \to \infty$ we recover the potential independent model from the conductance-based version, i.e., $U^{\text{CB}} \to U$, and the conditions for the different properties of U^{CB} become the conditions for U in Table B.1.

TABLE B.1
Properties of different rise functions. $\eta = E_{\mathrm{syn}}(\alpha - \beta)$.

U	Parameter domain	Concave	Convex	Sigmoidal	icpd	dcpd
U_{LIF}	$E_{\mathrm{eq}} > 1$	$\surd$	-	-	$\surd$	-
$U_{\mathrm{LIF}}^{\mathrm{CB}}$	$E_{\mathrm{syn}} > 1$, $E_{\mathrm{eq}} > 1$	$E_{\mathrm{syn}} > E_{\mathrm{eq}}$	$E_{\mathrm{syn}} < E_{\mathrm{eq}}$	-	$E_{\mathrm{syn}} \geq E_{\mathrm{eq}}$	$E_{\mathrm{syn}} \leq E_{\mathrm{eq}}$
U_{QIF}	$0 \leq \alpha < \infty$, $-\infty < \beta \leq 0$, $\alpha > \beta$	$\beta = 0$	$\alpha = 0$	$\beta < 0 < \alpha$	-	$\alpha \leq 1$, $-1 \leq \beta$
$U_{\mathrm{QIF}}^{\mathrm{CB}}$	$E_{\mathrm{syn}} > 1$, $0 \leq \alpha < \infty$, $-\infty < \beta \leq 0$	-	$0 \leq 1+\alpha(\alpha - 2\eta)$	$0 > 1+\alpha(\alpha - 2\eta)$	-	$\alpha^2 \leq \frac{\eta}{\eta-\alpha-\alpha^{-1}}$, $\beta^2 \leq \frac{\eta-\alpha+\beta}{\eta-\alpha-\beta^{-1}}$
U_b	$b \in \mathbb{R} \setminus \{0\}$	$b < 0$	$b > 0$	-	$\surd$	$\surd$

B.2. Icpd and dcpd rise functions. Usually it is difficult to verify the icpd or dcpd property of a rise function as given in Definition 3.8. Here we show that it is closely related to the third derivative of U.

We first note that ΔH obeys the relations $\Delta H(\phi, 0, \varepsilon) \equiv 0$ and $\Delta H(\phi, \Delta\phi, 0) \equiv \Delta\phi$ and hence $\frac{\partial}{\partial\phi}\Delta H(\phi, \Delta\phi, 0) = 0$ and

$$\frac{\partial}{\partial\phi}\Delta H(\phi, \Delta\phi, \varepsilon) = \int_0^{\varepsilon}\int_0^{\Delta\phi} \frac{\partial}{\partial\phi}\frac{\partial}{\partial\varepsilon}\frac{\partial}{\partial\Delta\phi}\Delta H\left(\phi, \tilde{\Delta\phi}, \tilde{\varepsilon}\right) \mathrm{d}\tilde{\Delta\phi}\mathrm{d}\tilde{\varepsilon}.$$

Thus U is icpd if

$$\frac{\partial^3}{\partial\phi\partial\varepsilon\partial\Delta\phi}\Delta H(\phi, \Delta\phi, \varepsilon) \geq 0 \quad \text{for all } (\phi, \Delta\phi, \varepsilon) \in \mathcal{D}. \tag{B.8}$$

Using $\leq$ instead of $\geq$ yields an analogous condition for dcpd U. By definition of ΔH (B.8) yields the condition

$$\begin{aligned}\frac{\partial^3}{\partial\phi\partial\varepsilon\partial\Delta\phi}\Delta H(\phi, \Delta\phi, \varepsilon) = {} & 3\frac{U''(H(\phi+\Delta\phi, \varepsilon))^2 U'(\phi+\Delta\phi)^2}{U'(H(\phi+\Delta\phi, \varepsilon))^5} \\ & - \frac{U''(\phi+\Delta\phi)U''(H(\phi+\Delta\phi, \varepsilon))}{U'(H(\phi+\Delta\phi, \varepsilon))^3} \\ & - \frac{U'(\phi+\Delta\phi)^2 U'''(H(\phi+\Delta\phi, \varepsilon))}{U'(H(\phi+\Delta\phi, \varepsilon))^4} \\ \geq {} & 0 \quad \text{for all } (\phi, \Delta\phi, \varepsilon) \in \mathcal{D}.\end{aligned}$$

Substituting $H(\phi + \Delta\phi, \varepsilon) \to \phi$ and $\phi + \Delta\phi \to \psi$, one obtains

$$U'''(\phi) \leq 3\frac{U''(\phi)^2}{U'(\phi)} - \frac{U''(\psi)U''(\phi)U'(\phi)}{U'(\psi)^2} \quad \text{for all } 0 \leq \psi \leq \phi \leq 1 \tag{B.9}$$

as a nonlocal sufficient condition for a rise function to be icpd. The condition for dcpd U is given when replacing $\leq$ by $\geq$.

Now note that if (B.9) is satisfied locally for $\phi = \psi$, the sign of the derivative

$$\frac{\partial}{\partial\psi}\left(3\frac{U''(\phi)^2}{U'(\phi)} - \frac{U''(\psi)U''(\phi)U'(\phi)}{U'(\psi)^2}\right) = U''(\phi)U'(\phi)\left(2\frac{U''(\psi)^2}{U'(\psi)^3} - \frac{U'''(\psi)}{U'(\psi)^2}\right)$$

is determined by $U''(\phi)$ since the term in brackets on the right-hand side at $\phi = \psi$ is positive using inequality (B.9) and $U' > 0$. Hence, if U is concave, a sufficient local condition for a rise function to be icpd is

$$U''(\phi) \leq 0 \quad \text{and} \quad U'''(\phi) \leq 2\frac{U''(\phi)^2}{U'(\phi)} \quad \text{for all } 0 \leq \phi \leq 1.$$

Conversely a local condition for a convex rise functions to be dcpd is given by

$$U''(\phi) \geq 0 \quad \text{and} \quad U'''(\phi) \geq 2\frac{U''(\phi)^2}{U'(\phi)} \quad \text{for all } 0 \leq \phi \leq 1.$$

Different properties of commonly used rise functions are summarized in Table B.1.

REFERENCES

[1] L. Abbott and C. van Vreeswijk, *Asynchronous states in networks of pulse-coupled oscillators*, Phys. Rev. E, 48 (1993), pp. 1483–1490.

[2] M. Abeles, *Time is precious*, Science, 304 (2004), pp. 523–524.

[3] B. E. Alger and R. A. Nicoll, *GABA-mediated biphasic inhibitory responses in hippocampus*, Nature, 281 (1979), pp. 315–317.

[4] N. Anderson, E. B. Saff, and R. S. Varga, *On the Eneström-Kakeya theorem and its sharpness*, Linear Algebra Appl., 28 (1979), pp. 5–16.

[5] P. Ashwin and M. Timme, *Unstable attractors: Existence and robustness in networks of oscillators with delayed pulse coupling*, Nonlinearity, 18 (2005), pp. 2035–2060.

[6] M. Banaji, *Clustering in globally coupled oscillators*, Dyn. Syst., 17 (2002), pp. 263–285.

[7] S. Bottani, *Pulse-coupled relaxation oscillators: From biological synchronization to self-organized criticality*, Phys. Rev. Lett., 74 (1995), pp. 4189–4192.

[8] S. Bottani and B. Delamotte, *Self-organized-criticality and synchronization in pulse coupled relaxation oscillator systems; the Olami, Feder, and Christensen and the Feder and Feder model*, Phys. D, 103 (1997), pp. 430–441.

[9] P. Bressloff, S. Coombes, and B. de Souza, *Dynamics of a ring of pulse-coupled oscillators: Group theoretic approach*, Phys. Rev. Lett., 79 (1997), pp. 2791–2794.

[10] P. C. Bressloff, *Dynamics of a compartmental model integrate-and-fire neuron with somatic potential reset*, Phys. D, 80 (1995), pp. 399–412.

[11] P. C. Bressloff and S. Coombes, *Dynamics of strongly coupled spiking neurons*, Neural Comput., 12 (2000), pp. 91–129.

[12] J. Buck, *Synchronous rhythmic flashing of fireflies.* II, Quart. Rev. Biol., 63 (1988), pp. 265–289.

[13] J. Buck and E. Buck, *Synchronous fireflies*, Sci. Amer., 234 (1976), pp. 74–85.

[14] A. Corral, C. J. Perez, A. Diaz-Guilera, and A. Arenas, *Synchronization in a lattice model of pulse-coupled oscillators*, Phys. Rev. Lett., 75 (1995), pp. 3697–3700.

[15] M. Denker, *Complex Networks of Spiking Neurons with a Generalized Rise Function*, diploma thesis, Department of Physics, University of Göttingen, 2002.

[16] M. Denker, M. Timme, M. Diesmann, F. Wolf, and T. Geisel, *Breaking synchrony by heterogeneity in complex networks*, Phys. Rev. Lett., 92 (2004), article 074103.

[17] B. Doiron, A.-M. Oswald, and L. Maler, *Interval coding* II. *Dendrite-dependent mechanisms*, J. Neurophysiol., 97 (2007), pp. 2744–2757.

[18] R. J. Elble and W. C. Koller, *Tremor*, Johns Hopkins University Press, Baltimore, MD, 1990.

[19] J. Engel and T. A. Pedley, eds., *Epilepsy: A Comprehensive Textbook*, Lippincott-Raven, Philadelphia, 1997.

[20] B. Ermentrout, *Type* I *membranes, phase resetting curves, and synchrony*, Neural Comput., 8 (1996), pp. 979–1001.

[21] G. B. Ermentrout and N. Kopell, *Parabolic bursting in an excitable system coupled with a slow oscillation*, SIAM J. Appl. Math., 46 (1986), pp. 233–253.

[22] U. Ernst, K. Pawelzik, and T. Geisel, *Synchronization induced by temporal delays in pulse-coupled oscillators*, Phys. Rev. Lett., 74 (1995), pp. 1570–1573.

[23] U. Ernst, K. Pawelzik, and T. Geisel, *Delay-induced multistable synchronization of biological oscillators*, Phys. Rev. E, 57 (1998), pp. 2150–2162.

[24] N. Fourcaud-Trocme, D. Hansel, C. van Vreeswijk, and N. Brunel, *How spike generation mechanisms determine the neuronal response to fluctuating inputs*, J. Neurosci., 23 (2003), pp. 11628–11640.
[25] G. Eneström, *Härledning af en allmän formel för antalet pesionärer*, Öfv. af. Kungl. Vetenskaps-Akademiens Förhandlingen, Stockholm, 6 (1893).
[26] R. F. Galan, G. B. Ermentrout, and N. N. Urban, *Efficient estimation of phase-resetting curves in real neurons and its significance for neural-network modeling*, Phys. Rev. Lett., 94 (2005), article 158101.
[27] W. Gerstner and J. L. van Hemmen, *Coherence and incoherence in a globally coupled ensemble of pulse-emitting units*, Phys. Rev. Lett., 71 (1993), pp. 312–315.
[28] W. Gerstner, J. L. van Hemmen, and J. D. Cowan, *What matters in neuronal locking?*, Neural Comput., 8 (1996), pp. 1653–1676.
[29] M. Golubitsky and I. I. Stewart, *Nonlinear dynamics of networks: The groupoid formalism*, Bull. Amer. Math. Soc. (N.S.), 43 (2006), pp. 305–364.
[30] D. Hansel and G. Mato, *Asynchronous states and the emergence of synchrony in large networks of interacting excitatory and inhibitory neurons*, Neural Comput., 15 (2003), pp. 1–56.
[31] D. Hansel, G. Mato, and C. Meunier, *Clustering and slow switching in globally coupled phase oscillators*, Phys. Rev. E, 48 (1993), pp. 3470–3477.
[32] D. Hansel, G. Mato, and C. Meunier, *Synchrony in excitatory neural networks*, Neural Comput., 7 (1995), pp. 307–337.
[33] J. J. Hopfield and A. V. Herz, *Rapid local synchronization of action potentials: Toward computation with coupled integrate-and-fire neurons*, Proc. Natl. Acad. Sci. USA, 92 (1995), pp. 6655–6662.
[34] R. A. Horn and C. R. Johnson, *Matrix Analysis*, Cambridge University Press, Cambridge, UK, 1996.
[35] A. Hurwitz, *Mathematische Werke*, Birkhäuser, Basel, Stuttgart, 1933.
[36] S. Kakeya, *On the limits of the roots of an algebraic equation with positive coefficients*, Tohoku Math. J., 2 (1912), pp. 140–142.
[37] C. Kirst, T. Geisel, and M. Timme, *Sequential desynchronization in networks of spiking neurons with partial reset*, Phys. Rev. Lett., 102 (2009), article 068101.
[38] C. Kirst and M. Timme, unpublished.
[39] C. Kirst and M. Timme, *From networks of unstable attractors to heteroclinic switching*, Phys. Rev. E, 78 (2008), article 065210(R).
[40] I. Z. Kiss, C. G. Rusin, H. Kori, and J. L. Hudson, *Engineering complex dynamical structures: Sequential patterns and desynchronization*, Science, 316 (2007), pp. 1886–1889.
[41] Y. Kuramoto, *Collective synchronization of pulse-coupled oscillators and excitable units*, Phys. D, 50 (1991), pp. 15–30.
[42] L. Lapicque, *Recherches quantitatives sur l'excitation electrique des nerfs traitee comme une polarisation*, J. Physiologie, 9 (1907), pp. 620–635.
[43] Z. Liu, Y.-C. Lai, and F. C. Hoppenstaedt, *Phase clustering and transition to phase synchronization in a large number of coupled nonlinear oscillators*, Phys. Rev. E, 63 (2001), article 055201.
[44] Y. Maistrenko, O. Popovych, O. Burylko, and P. A. Tass, *Mechanism of desynchronization in the finite-dimensional Kuramoto model*, Phys. Rev. Lett., 93 (2004), article 084102.
[45] D. A. McCormick and D. Contreras, *On the cellular and network bases of epileptic seizures*, Ann. Rev. Physiol., 63 (2001), pp. 815–46.
[46] M. L. Mehta, *Matrix Theory*, Hindustan Publishing, Delhi, India, 1989.
[47] R.-M. Memmesheimer and M. Timme, *Designing the dynamics of spiking neural networks*, Phys. Rev. Lett., 97 (2006), article 188101.
[48] R. E. Mirollo and S. H. Strogatz, *Synchronization of pulse-coupled biological oscillators*, SIAM J. Appl. Math., 50 (1990), pp. 1645–1662.
[49] Z. Olami, H. J. S. Feder, and K. Christensen, *Self-organized criticality in a continuous, nonconservative cellular automaton modeling earthquakes*, Phys. Rev. Lett., 68 (1992), pp. 1244–1247.
[50] S. A. Oprisan and C. C. Canavier, *The influence of limit cycle topology on the phase resetting curve*, Neural Comput., 14 (2002), pp. 1027–1057.
[51] D. H. Perkel, J. H. Schulman, T. H. Bullock, G. P. Moore, and J. P. Segundo, *Pacemaker neurons: Effects of regularly spaced synaptic input*, Science, 145 (1964), pp. 61–63.
[52] C. Peskin, *Mathematical Aspects of Heart Physiology*, Courant Institute of Mathematical Sciences, New York University, New York, 1984.

[53] A. Pikovsky, O. Popovych, and Y. Maistrenko, *Resolving clusters in chaotic ensembles of globally coupled identical oscillators*, Phys. Rev. Lett., 87 (2001), article 044102.
[54] P. F. Pinsky, *Synchrony and clustering in an excitatory neural network model with intrinsic relaxation kinetics*, SIAM J. Appl. Math., 55 (1995), pp. 220–241.
[55] O. Popovych, V. Krachkovskyi, and P. A. Tass, *Desynchronization transitions in coupled phase oscillator systems with delay*, in Proceedings of the 11th International Workshop on Nonlinear Dynamics of Electronic Systems (NDES 2003), R. Stoop, ed., University of Zurich, Zurich, Switzerland 2003, pp. 197–200.
[56] A. D. Reyes and E. E. Fetz, *Two modes of interspike interval shortening by brief transient depolarizations in cat neocortical neurons*, J. Neurophysiol., 69 (1993), pp. 1661–1672.
[57] J. Rinzel, D. Terman, X.-J. Wang, and B. Ermentrout, *Propagating activity patterns in large-scale inhibitory neuronal networks*, Science, 279 (1998), pp. 1351–1355.
[58] J. P. Rospars and P. Lansky, *Stochastic model neuron without resetting of dendritic potential: Application to the olfactory system*, Biol. Cybernet., 69 (1993), pp. 283–294.
[59] W. Senn and R. Urbanczik, *Similar nonleaky integrate-and-fire neurons with instantaneous couplings always synchronize*, SIAM J. Appl. Math., 61 (2000), pp. 1143–1155.
[60] W. Singer, *Striving for coherence*, Nature, 397 (1999), pp. 391–393.
[61] W. Singer and C. M. Gray, *Visual feature integration and the temporal correlation hypothesis*, Ann. Rev. Neurosci., 18 (1995), pp. 555–586.
[62] V. Sturm, T. Schlapfer, W. Klosterkotter, H. J. Freund, D. Lenartz, and P. A. Tass, *Deep brain stimulation—a neurosurgical approach to modulate brain function; its current use in neurological disorders; its promise in phsychiatric disorders*, Int. J. Neuropsychoph., 9 (2006), pp. S55–S56.
[63] P. A. Tass, *A model of desynchronizing deep brain stimulation with a demand-controlled coordinated reset of neural subpopulations*, Biol. Cybernet., 89 (2003), pp. 81–88.
[64] M. Timme and F. Wolf, *The simplest problem in the collective dynamics of neural networks: Is synchrony stable?*, Nonlinearity, 7 (2008), pp. 1579–1599.
[65] M. Timme, F. Wolf, and T. Geisel, *Coexistence of regular and irregular dynamics in complex networks of pulse-coupled oscillators*, Phys. Rev. Lett., 89 (2002), article 258701.
[66] M. Timme, F. Wolf, and T. Geisel, *Prevalence of unstable attractors in networks of pulse-coupled oscillators*, Phys. Rev. Lett., 89 (2002), article 154105.
[67] M. Timme, F. Wolf, and T. Geisel, *Unstable attractors induce perpetual synchronization and desynchronization*, Chaos, 13 (2003), pp. 377–387.
[68] M. Tsodyks, I. Mitkov, and H. Sompolinsky, *Pattern of synchrony in inhomogeneous networks of oscillators with pulse interactions*, Phys. Rev. Lett., 71 (1993), pp. 1280–1283.
[69] C. van Vreeswijk, *Analysis of the asynchronous state in networks of strongly coupled oscillators*, Phys. Rev. Lett., 84 (2000), pp. 5110–5113.
[70] C. van Vreeswijk, L. F. Abbott, and G. B. Ermentrout, *When inhibition not excitation synchronizes neural firing*, J. Comput. Neurosci., 1 (1994), pp. 313–321.
[71] C. van Vreeswijk and H. Sompolinsky, *Chaos in neuronal networks with balanced excitatory and inhibitory activity*, Science, 274 (1996), pp. 1724–1726.